The Thesis Committee for Xiaoran Li
Certifies that this is the approved version of the following thesis:

An Experimental Study of Compression Force Effect on Electrosurgical Tissue Welding

APPROVED BY
SUPERVISING COMMITTEE:

Supervisor:

Wei Li

Richard Crawford

An Experimental Study of Compression Force Effect on Electrosurgical Tissue Welding

by

Xiaoran Li, B.S.E.

Thesis

Presented to the Faculty of the Graduate School of

The University of Texas at Austin

in Partial Fulfillment

of the Requirements

for the Degree of

Master of Science in Engineering

The University of Texas at Austin

May 2015

Acknowledgements

I would like to express my sincerest gratitude to my advisor Prof. Wei Li. Without his support, guidance, patience and inspiration, both mentally and technically, I could never have made it this far. I am honored to be a member of his research group, which truly functions as a family.

I also would like to show my greatest respect and appreciation to Prof. Richard Crawford for serving as the second reader of this thesis. It was a great experience taking his Design Methodologies course and working with him.

Thanks to our research group members. Thanks you for all the insight and thoughts you guys brought during our group meetings. Without you, my thesis would have taken much longer to complete.

Many thanks to my colleagues and friends, especially Russell Borduin, Jingqiang Zha, Dongyi Zhou, Wei Jiang, Fenglin Fan, Zhefeng Lin and Jinsong Liu for helping me gain knowledge and skills in unfamiliar areas.

In the end, I want to express my deepest thanks to my parents for their faith and unconditional support for me. Love you as always.

Abstract

An Experimental Study of Compression Force Effect on Electrosurgical Tissue Welding

by

Xiaoran Li, M.S.E

The University of Texas at Austin, 2015

Supervisor: Wei Li

Electrosurgical devices, especially bipolar forceps, are widely used in modern surgeries. Despite the advantages of reduce blood loss, better efficiency and less fatigue compared to traditional tools, these surgical devices often cause problems such as sticking and unwanted damage to surround tissue when used for tissue welding. Through a literature study of commercially available bipolar forceps, it is found that the compression force between the jaws is non-uniform, which leads to inconsistent tissue joint quality. In this research, the effect of compression force uniformity is studied with a specially designed device to achieve uniform and consistent compression force between the jaws of a bipolar forceps. Tissue welding experiments were conducted with tissue mimicking material under both uniform and non-uniform compression forces. The results indicate that the uniform compression force could potentially lead to better joint quality, reduced risk of tissue charring and sticking, and reduced operation time. The experimental device developed in this research provides an important platform for future studies in joint quality monitoring and control for electrosurgical devices.

Table of Contents

List of Tables

List of Figures

CHAPTER 1. INTRODUCTION

1.1 Electrosurgical Devices

It has been decades since different kinds of energy sources were applied in clinical surgery operations and other surgical practices. With the development of technologies in engineering and scientific areas, more advanced machines are invented to offer a variety of choices for more and more complex operations with better quality. Devices that use electricity to heat tissue or part of itself, such as the tip or surface, have replaced those using laser as the most commonly used devices today [1-3]. Electrosurgery is the terminology describing the use of electrical-energy based devices to apply heat to tissue for cutting, coagulating, desiccating and fulgurating functions. Reducing the side effects, including unwanted thermal damage to surrounding tissues and jaw-tissue sticking, and enhancing their functionality and applications are the main challenges to the development of electrosurgical devices (ESD) [1-3, 5].

Generally speaking, an ESD unit consists of a generator that function as the power source and waveform generator, a handpiece that contains one electrode for a monopolar device or two electrodes for a bipolar forceps, and a hand/foot switch to turn on or off the current to electrodes. The prefix “mono” or “bi” indicates the number of electrodes in the handpiece. According to the working principle of electrosurgical devices, two electrodes are required to perform the electrosurgery. In a monopolar unit, a return pad is included to serve as the patient return electrode and

form a complete loop. Units with irrigation capabilities have a liquid container and one or two tubes connecting the container to the handpiece.

There are two different types of electrosurgical generators. The first uses a ground as part of the circuit, while the other is a solid-state generator that avoids connection between the return electrode and the ground. The solid-state generator has advantages in avoiding alternate site burns and return electrode burns since the current will always go back to the generator instead of finding a path with the minimal resistance.

Monopolar and bipolar devices have completely different handpieces. Monopolar units normally use a pencil shape handpiece with the electrode as the tip of the pencil. Usually, the switch for monopolar devices is on the handpiece, though some devices can be controlled by a foot switch. For bipolar forceps, there are two commonly adopted handpieces, but each has two jaw-like tips to clamp the target tissue and perform the electrosurgical operation. Figure 1.1 shows the two major types of bipolar forceps. The left is a tweezers-like forceps, while the right is a forceps with a long insertion tube for minimum invasive surgeries.

Figure 1.1 Two common types of bipolar forceps [4]

Most of bipolar forceps are controlled by a foot switch for ease of operation. Common functions that can be achieved on a bipolar forceps include cutting, clamping, and position lock and rotation for some devices. The Z-shape bipolar forceps shown on the left in Figure 1.1 is an example of forceps designed to increase convenience of application in different conditions. The Z-shape can provide a better view of the surgical site for the surgeon due to the arrangement of the tips and handle of the forceps. Other forceps may use curved tips for tissues with complex geometry.

The material used to fabricate the tips or the jaws of the bipolar forceps is stainless steel in most situations, especially for disposable ones. Materials such as gold and silver are also used in tips for better thermal conductivity and to achieve the non-stick feature. Mirror surface finish can also be helpful to reduce tissue sticking; however, the surface finish can be destroyed easily after several use-cleaning cycles [7].

1.2 Motivation

When bipolar forceps are used for tissue welding (coagulation) to seal vessels or wounds, the compression force on the tissue is mostly non-uniform, caused by the closing angle of the jaws. Figure 1.2 shows a close-up picture of a bipolar forceps (Therma-Sect 010713-01, Karl Storz GmbH & Co. KG). The bipolar forceps has an insulation tube that can be pushed forward, forcing the two steel jaws to close. When the tube is released, the jaws are open due to spring force. It can be seen from the picture that after the jaws are closed, there is still a gap in between due to the non-parallelism of the two jaws. This gap leads to non-uniform compression force along

the jaw surfaces during the tissue welding process. Since the clamping condition affects the electrical contact between the electrodes and the tissue, as well as at the tissue interface, this non-uniform compression force has a significant effect on tissue welding quality.

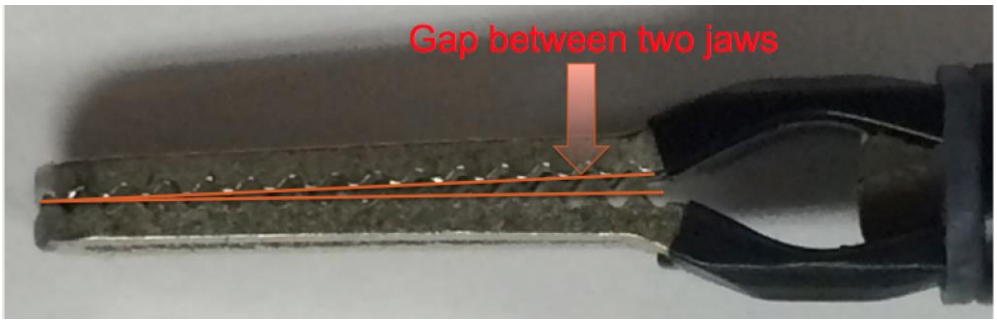

Figure 1.2 Gap between the jaws of a bipolar forceps

The effect of compression force of bipolar forceps has recently attracted much attention. Chastagner studied how compression force and water content level influenced the thermal conductivity of tissue [20]. It was found that the loss of air and fluids in the tissue, as well as the change of cellular structure, were the reason for drop in thermal conductivity. Dodde continued the research to quantify the relationship between the compression force and bioimpedance using porcine spleen tissue [17]. Although the above studies revealed the effect of compression force on tissue properties, it should be noted that the bioimpedance and thermal conductivity were obtained statically at fixed force levels. No welding was conducted during the measurements.

Chen attached a piezoresistive force sensor on the trigger of a bipolar forceps to study the force effect on tissue welding quality. Different force levels were applied

with three different bipolar forceps (with the same generator) to seal three different types of vessels. The force was applied by hand. Burst pressure was used as an indicator of the joint quality. It was found that a higher compression force would normally result in a higher burst pressure. However, this was not always true. For Carotid arteries, a higher compression force did not always lead to a higher burst pressure.

From the above studies it is obvious that the compression force has a significant effect on the performance of bipolar forceps and electrosurgical tissue welding. However, it is not clear whether the force effect is due to non-uniformity of the compression force across the jaws. As has been seen, when the jaws closes down on the tissue or vessel, the two surfaces are not parallel to each other, leading to uneven compression, thus non-uniform heating.

1.3 Objectives

The purpose of this study is to develop an experimental setup and evaluate the effect of uniform compression force in the electrosurgical tissue welding process. The objectives include:

- To design and fabricate an experimental device that can achieve uniform and consistent compression force across the jaws.
- To conduct tissue welding experiments and record real-time data including compression force, voltage and current.
- To analyze the compression force effect on tissue welding and compare the results from uniform and non-uniform compression force conditions.

An experimental setup that can achieve uniform and consistent compression force was designed, fabricated and applied to tissue welding experiments. For comparison, similar experiments were conducted with a traditional bipolar forceps device. Real-time force, voltage, and current data were recorded and analyzed to reveal the difference between the two welding conditions. Tissue mimicking material instead of porcine vessels was used in all the experiments.

1.4 Thesis Organization

Chapter 1 introduces the electrosurgical method and devices with an emphasis on bipolar forceps. Research motivation and objectives, and the proposed methods are discussed in this chapter. Chapter 2 reviews the history, advantages and disadvantages, and recent development of electrosurgical devices. Mechanisms of tissue sealing and sticking, as well as potential future developments are also included. Chapter 3 describes the development of an experimental setup to achieve uniform compression force, and the tissue mimicking material used in the tests. The experimental procedures to compare the effects of non-uniform and uniform clamping forces are also discussed. Chapter 4 is for results and discussion. The force sensor calibration procedure is presented. Real time force measurements for the uniform compression force case are discussed. Real time voltage and current data are compared between the traditional bipolar forceps and the experimental device developed in this study. Chapter 5 summarizes the work and provides conclusions of this study, as well as recommendations for future research.

CHAPTER 2. LITERATURE REVIEW

2.1 History of Electrosurgical Devices

William T. Bovie is commonly recognized as the father of the electrosurgery. While he is indeed the inventor of the first commercial electrosurgical device, the idea of using heat to perform certain surgical functions dates back to centuries ago. In ancient times, heated objects were widely used to obtain hemostasis in medicine. Shortly after the scientific discovery of electricity in 18th century, people started to apply it into medicine. A French biophysicist called D'Arsonoval discovered that when alternating current with frequency higher than 10 KHz is applied to human body, the current would not cause spasm, pain or burnt in the tissue. He also noted that the current increases the temperature, oxygen absorption and carbon dioxide elimination as it passes through the body [1,2].

Diathermy describes an electrically induced heat, which was created by Nagelschmidt, a German physician. He invented the diathermy machine capable of cutting, desiccation, and fulguration. Fulguration is a procedure, applies a needle-like electrode to destroy and remove tissue using high frequency alternating current. The first cited use of electricity in surgery was a treatment to a carcinomatous ulcer on the hand of a patient by a French physician called Joseph Rivere with a generator similar to Nagelschmidt's [1-3, 5].

By the 1920s, William T. Bovie invented the predecessor of modern electrosurgical units, and Dr. Harvey Cushing performed the first use of this electrosurgical unit on October 1st, 1926 at a hospital in Boston, MA. An enlarging vascular myeloma from a patient's head was removed during the operation. This kind of unit was applied in practice for a long time, until ValleyLab developed a more compact version of it in 1967 [2, 3].

As time goes by, development in electrosurgical devices has brought bipolar forceps, coating material, irrigation system, solid-state generator, real-time tissue monitoring and other technologies into the modern electrosurgery unit. Some of the companies, e.g., Intuitive Surgical, Sunnyvale, CA, also tried to accomplish robotic assisted laparoscopic electrosurgery. Bipolar units have shown better performance in tissue welding operations, while monopolar units are mostly used for cutting and dissecting [5, 12-14].

2.2 Working Principles of ESD

Electrosurgical devices use high frequency alternating current, normally from 200 KHz to 3.3 MHz, to pass through tissue, so that the desired clinical effects can be achieved. Figure 2.1 shows an example of the function of AC of different frequencies [2]. The generator provides the power and the current is passed to the tissue through the electrode in the handpiece. Ideally, all the resistance is from the tissue, while in the real situation there are unintended resistances in the circuit such as the electrode-tissue interface impedance. After passing through the tissue and generating heat, the current will go back to the generator or to the ground to complete the circuit loop.

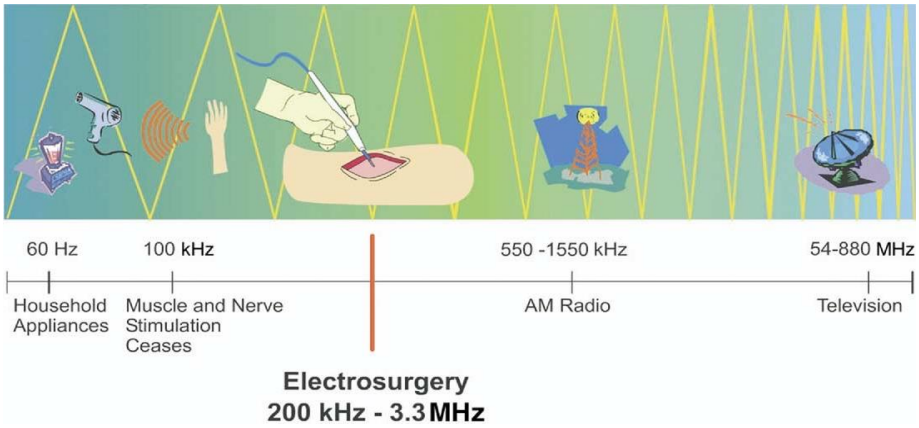

Figure 2.1 Functions of AC of different frequencies [5]

Within the range of 200 KHz to 3.3 MHz, waveforms with different patterns and settings are used for different operations. Figure 2.2 shows functions of different waveform patterns, or "modes". The left most is for pure cutting and the right most is for coagulating [2]. Cutting uses continuous sine waves while coagulating only needs 6% of the time required by cutting. The cutting process uses low voltage and high current while coagulating delivers power in the opposite manner but with the same amount of energy. In between the cutting and coagulating is the blend waveform, which is applied when hemostasis is needed during cutting.

In cutting mode, the low voltage (between 50 – 80 volts) and high current continuous waveform can increase the local tissue temperature to over 100 degrees Celsius and vaporize the tissue. For coagulating mode, the tissue is energized for a very short time and reaches a lower temperature. The tissue is heated only during the duty cycle and cools down during the remaining 94% of the total time so that coagulation occurs [1, 2, 5].

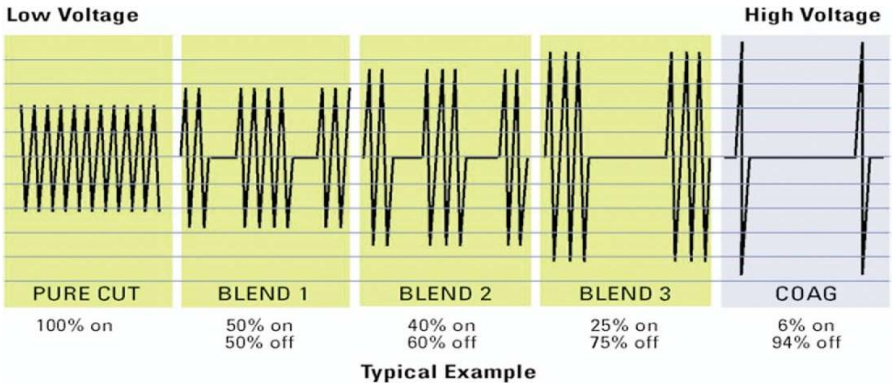

Figure 2.2 Patterns and power settings of different functions [2]

The difference in working principle between the monopolar and bipolar unit is the path of the current in the circuit. For the monopolar unit, current is delivered by the active electrode, which is the one in the handpiece, and the current finds the path of least resistance and returns to the generator or ground by the patient return pad under or attached to the patient body. For the bipolar forceps, the active and return electrode is in the handpiece, therefore the current will only travel through the tissue between the two tips. As can be seen, the monopolar device has more untargeted tissue involved in the loop, increasing the risk of unwanted damages. There are fewer side effects with bipolar devices and the post-operation recovery time is usually shorter.

2.3 Mechanisms of Tissue Sealing and Sticking

To get a better picture of the ESD, mechanisms of tissue sealing and sticking should be discussed. During the procedure for vessel sealing, the jaws of the ESD hold and compress the vessel tightly. This clamping action fixes the location where the procedures will be conducted and prevents the flux of blood from absorbing the heat generated within the operation site [15].

After the power is turned on, heat will be generated in the tissue due to bio-impedance. When the temperature around the site reaches 50℃, cell death occurs after about 6 minutes. Cell death could occur immediately when the temperature reaches 60℃. The bonds between protein molecules will be influenced by temperature within the range of 65℃ to 90℃. Homogenous coagulum, which is also known as coagulation, is formed by protein molecules bonds' reforming quickly after breaking. The homogenous gelatinous structure, which is formed by reforming of protein bonds, occludes blood vessels so that hemostasis can be achieved. Both the collapsed internal laminae and coagulated thrombus within the vessels contribute to vessel hemostasis caused by electrosurgery [15, 16].

Tissue sticking to electrodes, which is an area lacking of academia research, is mainly caused by excessive heat. Carbonized molecules and some sugar are generated near the electrode when the temperature reaches 200℃, causing adherence of the tissue to the electrode. This may lead to damage of sealed joint and cause bleeding or even total seal failure [15].

There are several ways to avoid sticking. Munro stated in his work that the use of continuous "cutting" waveform instead of pulsed "coagulation" waveform reduced the chance of sticking. Part of the reason is that the pulsed waveform leads to coagulation of superficial layers, which increases the impedance of tissue. This causes the heat to stay at superficial layers instead of transmitting into tissues. Another way of preventing sticking is to keep the electrode clean. Surfaces with accumulated coagulation tend to stick more than clean surfaces. Quantification of how sticking is influenced by compression force and temperature or other physical properties is a topic that needs further investigation [15].

Joint quality is normally measured by burst pressure. Dodde attempted to find correlation between the compression force and joint quality in his dissertation. According to his experiments, there should be an optimal compression force for different tissues. Not all the vessels will have a higher burst pressure with an increase in compression force. Other factors that can influence the joint quality include temperature, waveform from the generator, voltage and current level [17].

2.4 Advantages and Disadvantages of ESD

The advantages of electrosurgical devices have made them one of the most-commonly used surgical tools today. The blend waveform provided by the generator can dissect tissue and simultaneously achieve hemostasis. The quality of vessel sealing has improved with the development of devices. Burst pressure is used as the indicator of the sealing quality of vessels sealed by electrosurgical devices. These devices are clinically equivalent to other traditional methods such as clips and sutures in terms of burst pressure. While scalpel is the most commonly used tool for opening skin in surgery, recent applications of electrosurgical devices shows promising results in opening or cutting tissues both superficially and deep. Less blood loss is one big advantage of electrosurgical devices over the scalpel. The integrated design with bipolar forceps, foot switch and cutting blade for the modern bipolar forceps reduces the time and procedure of exchanging tools during the operation. Generally, electrosurgical devices provide an option with much higher ease and efficiency compare to traditional tools [2, 5, 6].

The downside of electrosurgical devices includes but may not be limited to the following: alternate site burns, capacitive coupling, damage to devices implanted to the patient and cost. The alternate site burn happens with monopolar electrosurgery when there is any insulation failure or improper grounding. If insulation failure occurs, stray current from the generator will find an alternate pathway to go back to the ground. If the current density is high or the resistance is low enough, alternate site burn will occur. Capacitive coupling is not avoidable but only happens in some certain situation. A capacitor is formed by two conductive parts separated by an insulator. During some operations, an active electrode is put down into a trocar forming capacitive coupling. The problem is worsened when the electrode is activated before it reaches the target tissue. Once the trocar has contact with tissues the energy stored will be released, causing damage and injuries. Although capacitive coupling is not avoidable, a conductive trocar provides a larger area for the energy to be dissipated so as to minimize the damage. The damage to devices implanted to the patient is easy to understand, but this only occurs for monopolar electrosurgery. If the patient has devices implanted in the body, the return electrodes should avoid the places where the devices are implanted. The cost for all the devices in the unit is high at the same time many of them are disposable, this will increase the fee for operations [1, 2, 5].

2.5 Recent Development of ESD

The research and development of electrosurgical devices attracts more and more attention from both academia and industry. Based on clinical needs of electrosurgical devices, many new techniques and inventions have been applied in each component of the unit. Mikami, et al., showed that gold-plated bipolar forceps

had minimal adherence of tissue during the coagulation process, while providing the most uniform histological changes to the tissue coagulated. They compared the performances in coagulation among mirror-surface-finished stainless steel, titanium, and gold bipolar forceps. The results contributed to the non-sticking feature of the ESD. Conductive material with high thermal diffusivity and conductivity while non-toxic to human body can be applied to fabricate the tips of bipolar forceps. With the high thermal conductivity and diffusivity, the heat in the tips can dissipate quickly enough before the temperature rising too high. Other factors that will influence the performance of coagulation include ionization tendency of the tip material, electrical distribution on the tip surface and the wetting tension of the material [7].

Blade or tip coatings have been developed to prevent sticking of tissues to the tips. Konesky listed seven properties that a functional blade coating must have, which are: biocompatibility, conductivity, low surface energy, and good adhesion to blade, being able to withstand sterilization processes, durability and inexpensiveness. Usually the substrate of the blade is made of 300 or 400 series stainless steel to reduce cost, while the coating material can vary from metals like gold to composites like PolyTetraFluoroEthylene (Teflon). Ou, et al., also showed that units equipped with coated (chromium nitride) blades or tips have a better performance in non-stick and reducing thermal injury than those left untreated. Comparison between the CrN and another promising coating should also be conducted [8, 9].

According to the recent research, the main issues in coating are biocompatibility and adhesion to substrate material. Teflon was once regarded as an effective coating material for electrodes based on Ceviker et al.'s work. However, it discharges toxic particles when the temperature is too high during operations. More

work has shown that new Teflon coatings can generate highly toxic particles. The coating material may have different coefficients of thermal expansion, which will lead to cracks and failure of the coating. A “perfect” coating material is not available yet [8-11].

As the generator determines the waveform and power setting delivered to the handpiece, development of generator technology is also critical to electrosurgery. The basic trend of the development in generators is lower output impedance and power with more intelligent control. With the same working principle, different generators with different purposes were developed. Some generators with output power as low as 15 W, NS2000 (Valleylab, Boulder, CO) were developed for the purpose of neurosurgical procedures. Other examples include generators for coagulation only and those capable of bipolar cutting [12].

2.6 The Effect of Compression Force of Bipolar Forceps

Recently, the effect of compression forces of bipolar forceps has attracted much attention. Chastagner studied how compression force and water content level influences the thermal conductivity of tissue [20]. A device consisting of two clamping plates, a linear extensometer, a thermistor and a load cell was designed and assembled to measure how the thermal conductivity changes with different compression forces. Spleen tissue from mongrel canines was used for the test. The experiments showed that the thermal conductivity decreased by 12% with a joint influence of 64% water desiccation and the 70% tissue compression; with only 69% tissue compression, the thermal conductivity fell by 9%. Although the loss of air and fluids in the tissue, as well as the change of cellular structure, were believed to be the

reason for the drop in thermal conductivity, quantitative studies have not been conducted [20].

Dodde continued the research to quantify the relationship between compression force and bioimpedance using porcine spleen tissues [17]. With 80% strain the intracellular resistance increased by as much as 100%. This bioimpedance change was due to mass exudation from the intracellular space of compressed tissue material. Although the measurements revealed the effect of compression force, it should be noted that in both of the above studies, bioimpedance and thermal conductivity were obtained statically at different force levels. No welding was conducted during the measurements.

Chen fixed a piezoresistive force sensor on the handle or trigger of the bipolar forceps. Four different force levels were applied to the handle and corresponding compression forces between the jaws were recorded. The force applied at the handle was recorded and used as the indicator of the force applied between the jaws. Then these four different force levels were applied with three different bipolar forceps (with the same generator) to seal three different types of vessels, which were carotid arteries (4-6mm), femoral arteries (4-6mm) and jugular veins (2-4mm). Hand was used as the force input of the forceps. Figure 2.3 demonstrates the change of force during one application cycle. Sealing time and force at the handle were applied by an experienced surgeon [21].

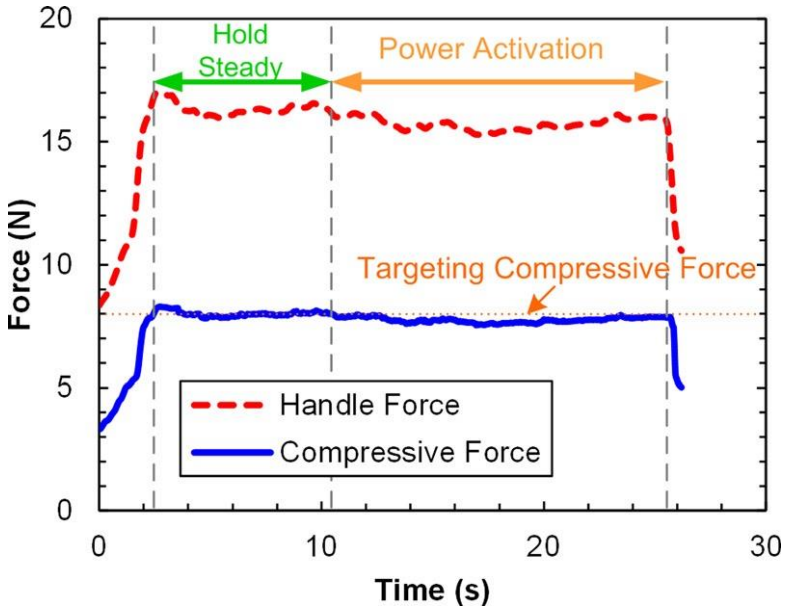

Figure 2.3 Force applied to handle and corresponding compression force of a jugular vein [21]

The burst pressure was used as the indicator of quality of the joint sealed during the experiments. It is found that a higher compression force will normally result in a higher burst pressure. However, this is not always true. Figure 2.4 shows that for Carotid Arteries, a higher compression force does not always lead to a higher burst pressure. Based on this result, Chen predicted that an optimal compression force could be found for each kind of vessels [21].

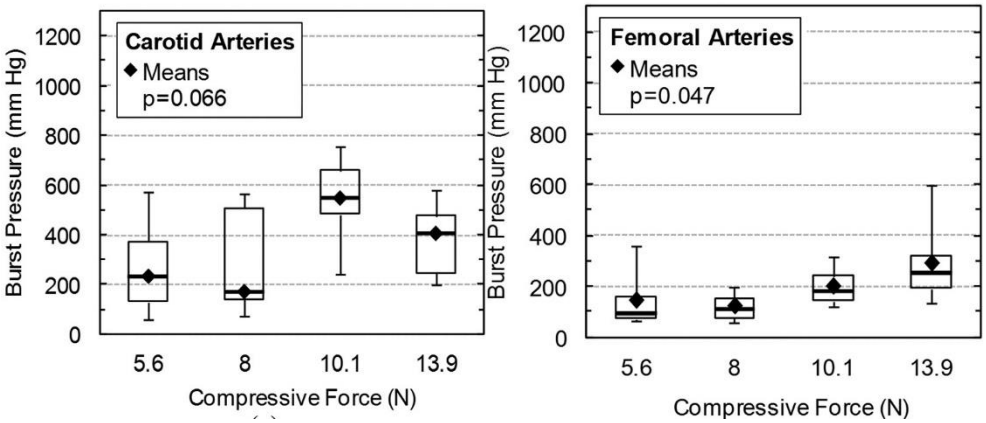

Figure 2.4 Burst pressure of four force levels:

carotid arteries on the left; femoral arteries on the right [21]

From the recent studies it is obvious that the compression force has a significant effect on the performance of bipolar forceps and electrosurgical tissue joints. However, it is not clear whether the force effect is due to non-uniformity of the force distribution across the jaws. As it has been seen in Chapter 1, when the jaws closes down on the tissue or vessel, the two surfaces are not parallel to each other, leading to uneven compression, thus non-uniformity heating. The purpose of this study is to develop an experimental setup and evaluate the effect of non-uniform compression force in the electrosurgical tissue welding process, such that significant improvement on joint quality can be achieved through future research on jaw design and process control.

CHAPTER 3. EXPERIMENTAL SETUP AND PROCEDURES

3.1 Introduction

In this chapter, the design and fabrication processes of an experimental setup to achieve uniform and consistent compression forces are introduced. The jaws of a commercial ESD handpiece were cut and fixed onto two insulator blocks. Holes were drilled in the insulator blocks. Ejector pins were fit through the holes to guide and ensure the parallel movement of the insulator blocks. Standard weights were used to generate the compression force between the two jaws. A piece of aluminum plate was used as a weight holder. Standard weights were placed in the center of the weight holder with marked position to ensure symmetric load distribution and repeatability. A flexible thin film force sensor was fixed in between the lower insulation block and the base plate to measure the force achieved between the jaws. It was assumed that the friction between the lower insulation blocks and the guiding rods is negligible. The entire setup was mounted on an optical breadboard.

In the second half of this chapter, the experiments conducted to compare the designed device and traditional bipolar forceps are described. Tissue mimicking material for human liver tissue was used for all the experiments. Voltage and current for the first 2 ms of every welding cycle was recorded for both the designed device and traditional bipolar forceps. Real-time forces for all complete cycles were measured only with the designed device. Fabrication of tissue mimicking material is also described in this chapter, followed by a description of experimental procedures. The repeatability of the designed device is discussed.

Figure 3.1 shows a schematic of the experimental setup with a specially designed device to achieve parallel jaw movement in the clamping and welding process. Force, voltage, and current were measured during the welding cycle. An oscilloscope (Tektronix MDO 3014 mixed domain, Beaverton, Oregon) with voltage and current probes was used to record the voltage and current. A force sensor (Tekscan, Inc., FlexiForce A201, South Boston, MA) was inserted under the lower insulator blocks to record the real-time force during the welding cycle via a cRio and LabVIEW (National Instruments, Austin, TX) on a PC. The jaws were powered by a generator (ConMed Corporation, Sabre 2400, Utica, NY) with 35 watts power setting for all the tests.

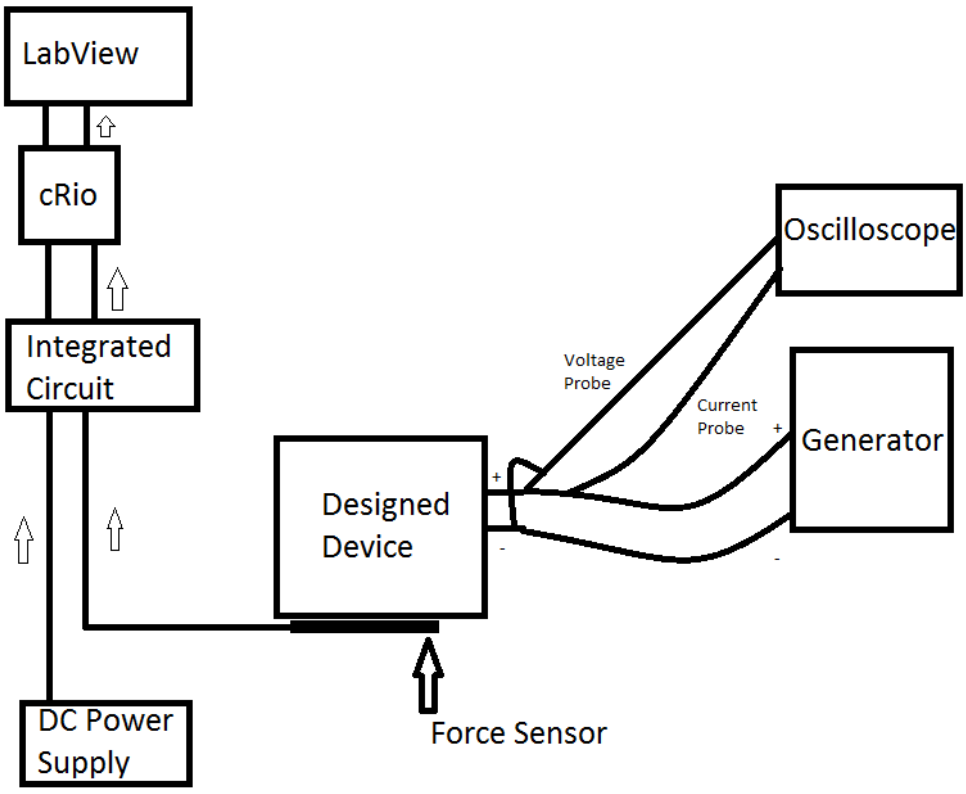

Figure 3.1 A schematic of the experimental setup

3.2 Fixture Design and Fabrication for Uniform Compression Force

3.2.1 FIXTURE DESIGN

Two designs of the device are considered to achieve a uniform and consistent compression force. The first is to integrate ESD jaws into a vise, since the motion of the vise jaws are constrained to be parallel. However, this design is hard to ensure consistent compression forces, because during the welding cycle of the bipolar forceps the tissue clamped between the jaws will heat up and expand. It can also shrink after the cycle is complete due to the vaporization of water. Therefore, the force during and after welding will be affected by the starting location of the vise jaws and is not consistent to the practice of tissue welding, where force instead of displacement is applied.

In this research, standard weights are used to achieve the compression force. Figure 3.2 shows a CAD model of the fixture design. Not shown in this CAD model are three holes drilled in the base plate to fix the setup to an optical breadboard. The key components are two insulation blocks where the ESD jaws are mounted.

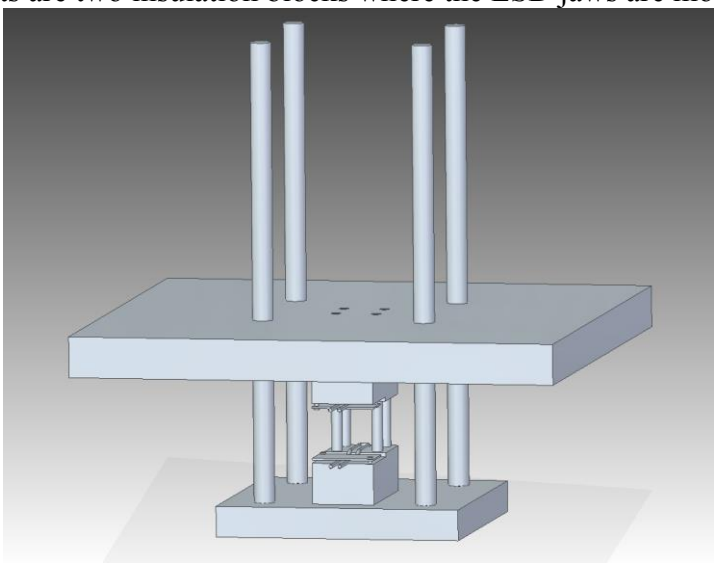

Figure 3.2 A CAD model of the fixture used for uniform compression force

Figure 3.3 shows the design of a complete insulation block with a jaw fixed on it. Design of the insulation block is crucial to the whole device, which needs to ensure the center of mass is sit on the center of jaws, so that undesired bending moment could be eliminated. The four holes in the block were drilled with a # 30 drill bit so that four inner ejector pins can be inserted. In Figure 3.3, the higher plane is the jaw plane and the lower plane is the fixing plane. The reason to have a step on the insulation block is the curved design of the commercially available jaws used in this study. The size of the jaw plane is 0.75 x 0.75" with the jaw sitting in the middle and the tip of jaw reaches 0.6" from the edge into the plane. The material used to machine the insulation block is Teflon. A fixing plate is used to fix the location of the jaws with the help of two size 0 screws. The material of the fixing plate is PEI (Polyetherimide) with a glass transition temperature (T_g) of 193.9 - 232.8 degrees Celsius, which is higher than the normal operating temperature (around 100 degrees Celsius) of the jaws [15, 23]. A 3/64* drill bit was used to drill the holes for the fixing screws. The tapping process was finished by a # 0 tap by hand, because a normal tap handle is too heavy for the holes and can damage them easily. Both insulation blocks have the same pattern for the fixing screws, so that when they are closed there will be no screws touching each other to short the circuit.

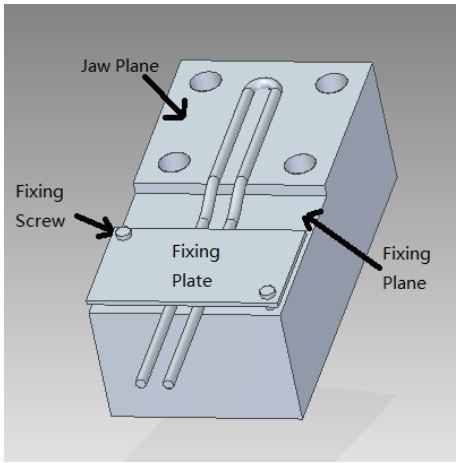

Figure 3.3 A CAD model of a complete insulation block

The weight holder is an aluminum block that can hold multiple weights to achieve different levels of force. The locations of all the holes are the same as those on the base plate. Figure 3.4 shows the setup with a 300 g standard weight on the weight holder.

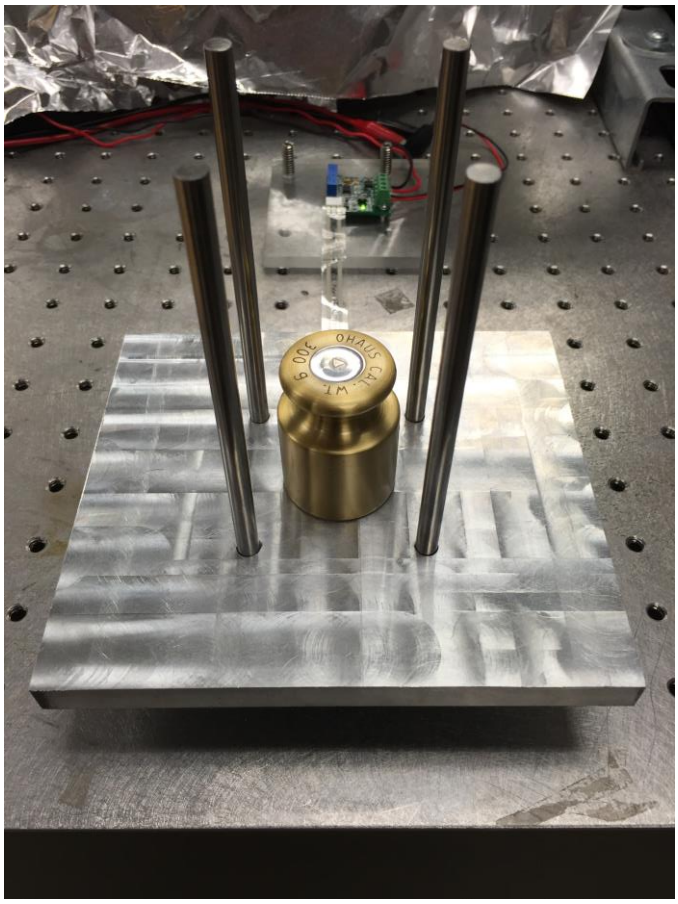

Figure 3.4 The weight holder with a 300 g standard weight on it

3.2.2 FIXTURE FABRICATION

A bill of material of the whole fixture setup is shown in Table 3.1. The precision ejector pins, also known as pin blanks, forged pins and pilot pins, are the key components of the device. The tolerance of the pins is -0.0005” to -0.0008”, so that they can ensure the straightness and the parallel movement of all the components.

The inner four pins are aimed to ensure the movements of the insulation blocks, so that the jaws can move straight up and down. The outer four pins are designed to secure the movements of heavier components including the weight holder and standard weights. They help prevent undesired bending of the inner ejector pins. The ejector pins were purchased from McMaster-Carr.

Table 3.1 Bill of material of the sample fixture

Specification / **Item Name**	**Dimensions**	**Material**	**Quantity**
Base Plate	3*3*3/8 inch	Aluminum	1
Small Ejector Pin	D_s = 1/8 inch* D_h = 1/4 inch* T_h = 1/8 inch* L_s = 40 mm*	Stainless Steel	4
Large Ejector Pin	D_s = 1/4 inch D_h = 7/16 inch T_h = 3/16 inch L_s = 6 inch	Stainless Steel	4
Insulation Block	1.5*3/4*1/2 inch	Teflon	2
Fixing Plate	3/4*1/2*1/20 inch	PEI	2
Fixing Screw	Size 0, ¼ inch length	Stainless Steel	4
Weight Holder	6*6*0.5 inch	Aluminum	1
Standard Weight	300g/500g/872.5g	Stainless Steel/Brass	3

* s stands for shaft, h stands for head, T stands for thickness, and L stands for length.

Figure 3.5 shows a CAD model of the base plate. The four inner through holes were drilled with a #30 drill bit. The major diameter of the # 30 drill bit is 0.1285". The four outer through holes were drilled with an F drill bit with a major diameter of 0.257". The counter sink holes for the inner ejector pins were finished with a quarter inch end mill, with the depth controlled to the same height of the inner pin head, which was 1/8 inch. The four larger counter sink holes were for the heads of the outer ejector pins. An end mill with a 7/16 inch diameter was used to finish the holes with a depth of 3/16 inch. The center point of the plate was marked as (0, 0) while the four outer holes' centers were marked as (±1, ±1) and the centers of the four inner holes (±0.25, ±0.25), with inch as the unit of all coordinates.

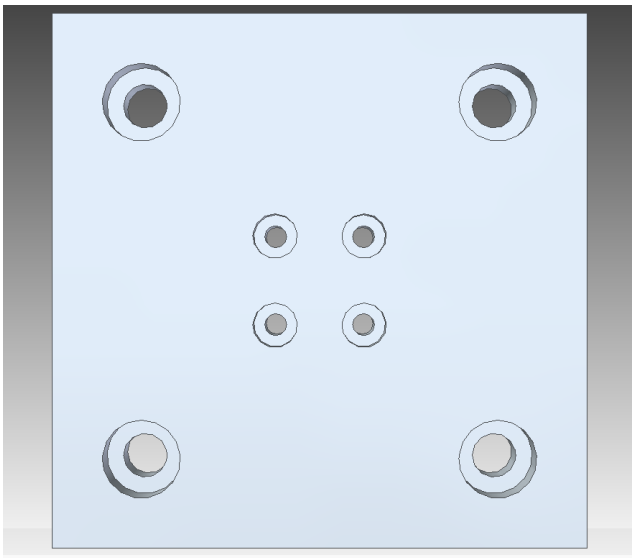

Figure 3.5 Bottom view of the base plate

Before drilling each hole, a size # 1 center drill was used to mark the position and reduce the error caused by the bending of drill bits. Rimmer, file and sand paper were used after all the machining processes to de-burr the edges and improve the surface finish. All the milling and drilling were conducted on a Bridgeport milling

machine in the Machine Shop of the Department of Mechanical Engineering, UT Austin. The same machine was used to reduce bias error that could be caused by using different machines.

3.3 Fixture for Non-uniform Compression Force

For traditional bipolar forceps, a setup shown in Figure 3.6 was used to achieve the compression force for operation. In this setup, the trigger of the bipolar forceps was squeezed using a vise. The vise was fixed on an optical breadboard. The force sensor was inserted in between the moving clamp of the vise and the hand trigger of the forceps. A piece of foam was wrapped over the contact surface of the handle to enlarge the contact area of the sensor.

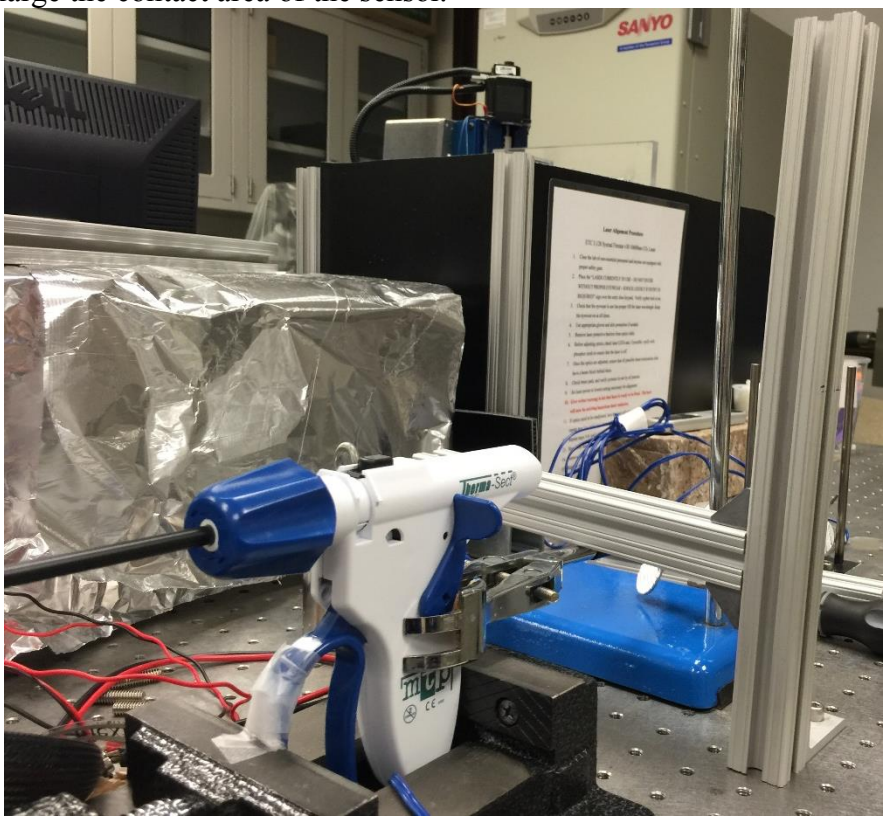

Figure 3.6 The setup for achieving compression force for traditional bipolar forceps

3.4 Tissue Mimicking Material

The fabrication of tissue mimicking material in this experiment was based on a procedure described in [25]. The materials needed for making the tissue mimicking material, or phantom material, included gellan gum, propylene glycol (PPG), 0.9% NaCl solution, deionized water, and sodium propionate. A more detailed BOM of the phantom material is shown in Table 3.2. Chen validated the feasibility of fabricating a phantom material based on high-acyl gellan gum to reproduce material with similar mechanical properties to a variety of real tissues. The step-by-step procedure for making 50 g of phantom material was developed as follows. All the ingredients were added in a plastic container according to the following order: 2.35 g of high-acyl gellan gum, 0.125 g of sodium propionate, 4.3 g of PPG, 32.275 g of deionized water and 10.45 g of 0.9% NaCl solution. The mixture was manually stirred until fully dissolved. The solution was then set for 15 minutes with cover. After that, the material was heated for 40 minutes in an oven at 110 degrees Celsius. The material was removed and cooled for three hours after heating [25]. In this study, a thin layer of phantom material was needed for the experiments. Therefore, stirring was not performed during the heating process as described in Chen's procedure. Instead, two pieces of glass were used to shape the material before loading into the oven. Figure 3.11 shows the material after it was cooled for three hours.

Table 3.2 Bill of material for tissue mimicking material

Item	Brand/ Source	Price
Gellan Gum	Mordenist Pantry	$57.99/400g
Propylene Glycol	Essential Depot	$10.95/Quart
0.9% NaCl Solution	Made at Lab	/
Deionized Water	Made at Lab	/
Sodium Propionate	Sigma-Aldrich	$30/500g

Figure 3.7 Phantom material after cooling for three hours

After cooling, the material was cut into small pieces with approximately 6 mm x 6 mm x 1 mm dimensions. Two pieces were stacked together to simulate the sealing process. All experiments were conducted with the same batch of phantom material, in order to reduce the error caused by batch to batch variation.

3.5 Data Acquisition

Real-time force, current, and voltage data were recorded in this study to compare the effects of uniform and non-uniform compression forces on electrosurgical tissue welding. Figure 3.8 shows the setup for data acquisition. The force sensor was powered with a circuit board (Tekscan, Inc., FlexiForce Quickstart Board, South Boston, MA), which converted the signal to 0 to 5 V. An oscilloscope was used to record the voltage and current data. The trigger of the measurement on the oscilloscope was set to 0 V and a sampling rate of 500 MHz was used. A total of 1 million data points were recorded for both voltage and current. Therefore, only the first 2 microseconds of data were recorded for each weld.

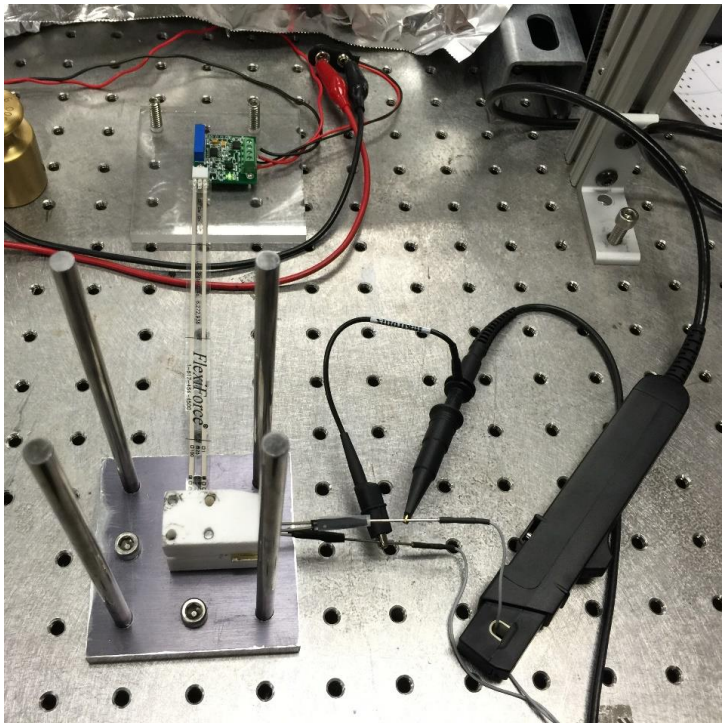

Figure 3.8 Setup for force, voltage, and current measurements

Real-time force data was recorded with a National Instrument data acquisition system, cRio. A LabVIEW VI was created as shown in Figure 3.9. The sampling rate of the cRio was set to 1000 Hz, while the sampling rate of the VI was set to 100 Hz.

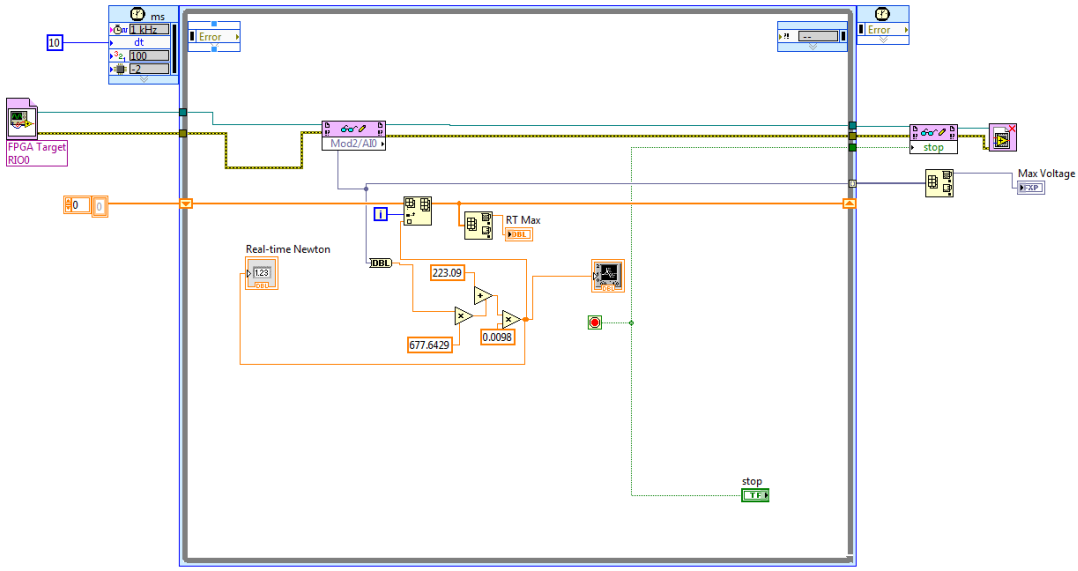

Figure 3.9 A screen shot of LabView VI for data acquisition

For experiments with traditional bipolar forceps, the force sensor was attached to the handpiece. The voltage leads were directly attached to the ESD jaws through extension wires. The dimensions of the jaws with teeth were 15 mm x 4 mm x 1 mm. In order to avoid shorting the circuit, each jaw was connected to an extension wire so that the voltage probe can be attached. Figure 3.10 shows the setup.

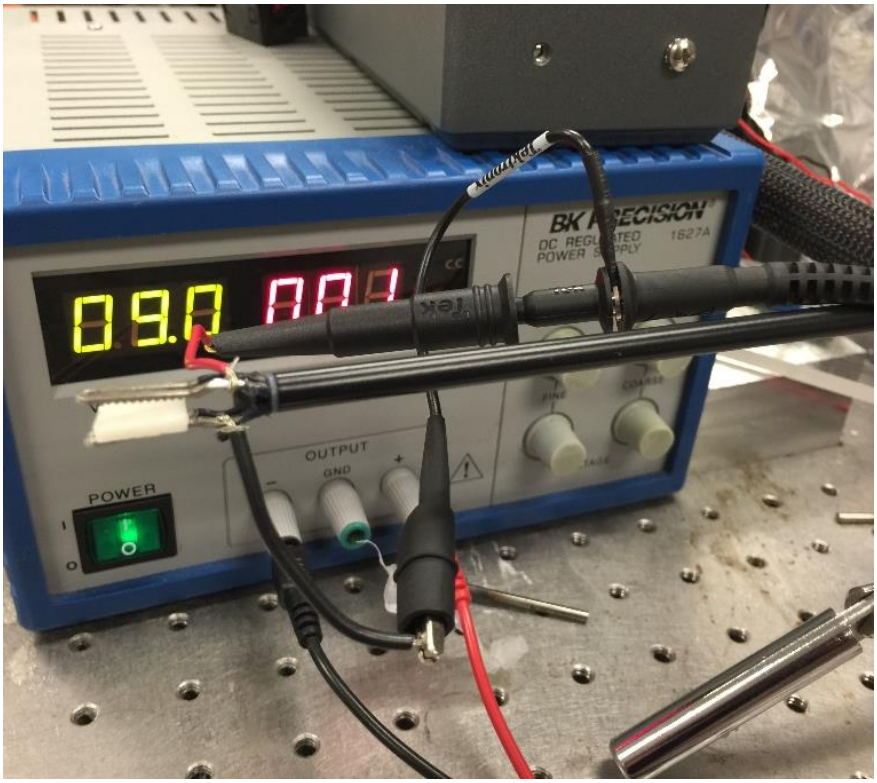

Figure 3.10 Voltage probe setup on the jaws

3.6 Experimental Procedures

3.6.1 CALIBRATION OF FORCE SENSORS

Before conducting the experiments, the force sensors need to be calibrated. Figure 3.11 shows the calibration setup for the uniform compression force case. Standard weights were applied and voltages were read from the NI DAQ system. The first force level was set to be 6.47 N, which was just the weight of the holder. The second force level was the weight holder plus the 300 g standard weight, which was 9.41 N in total. The third force level was the weight holder plus the 872.5 g standard weight, which was 15.02 N in total. The last force level was the weight holder with all the standard weights, giving a total of 22.86 N. Figure 3.11 shows a calibration step with the weight holder and a 300 g standard weight.

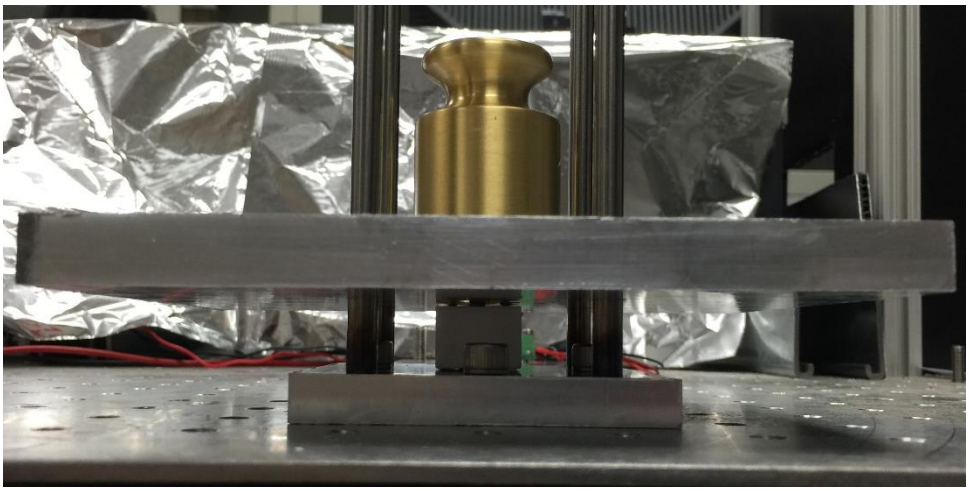

Figure 3.11 Calibration setup for the designed device

The calibration setup for the sensor used on the traditional bipolar forceps was the same except the sensor was different. The third and fourth force levels were different, which were 11.37 and 15.02 N, respectively. In order to find the force profile across the jaws for a traditional bipolar forceps, the sensor was trimmed smaller than the one used in the uniform compression case, such that multiple points can be measured across the jaws. The force sensor only outputs the maximum force it reads within the sensing area.

3.6.2 COMPARISON EXPERIMENTS

For experiments with a uniform compression force, two pieces of phantom material with approximately 6 mm x 6 mm x 1 mm dimensions were stacked and loaded in between the jaws to be sealed, as shown in Figure 3.12. The white materials in the center of the jaws are the phantom material. The force recording began after the standard weight was loaded on the weight holder. After 10 seconds when the force reading stabilized, the footswitch was stepped and held for 15 s, so that the power was turned on and transferred to the tissue. The heating was stopped approximately 25 s

after force recording was started. The force data acquisition was stopped until a constant output was reached. After each welding cycle where a constant force reading was reached, the load was removed immediately. Then the material was removed and the jaws were allowed to cool for 1 minute before starting the next test.

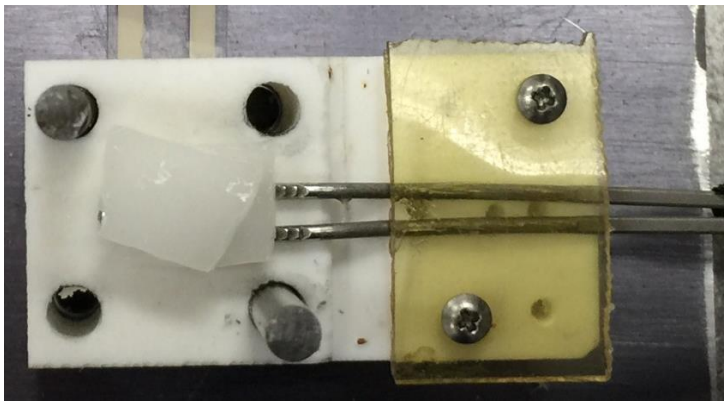

Figure 3.12 Two pieces of the phantom material in between the jaws to be welded

Three force levels were selected based on the availability of standard weights and levels used in literature [21]. The weight of the weight holder itself is 660 g, which exerts 6.47 N of force. There are two standard weights used in the experiments, the weights of which are 500 g and 300 g (4.9 N and 2.94 N), respectively. The three force levels were set to 6.47 N as the low level, 9.41 N as the medium level and 14.31 N as the high level. For each force level, the experiment was repeated three times for data analysis and verification. The power generator was set to 35 W for all the experiments. The length of the welding cycle and the power setting was adapted from [21].

For experiments with traditional bipolar forceps, the force was measured at the moving clamp of the vise instead of the jaws. Same as the uniform compression force experiments, two pieces of tissue mimicking material were inserted in between the jaws. After the force reading reached the target values (the same as the uniform

compression case) and stayed constant for 10 seconds, the footswitch was stepped and held for 15 seconds. The voltage and current data were recorded for the first 2 ms. After each welding cycle, the jaws were opened immediately. Then the material was removed and the jaws were allowed to cool for 1 minute before starting the next test. Each force level was repeated for three times.

3.7 Summary

This chapter discussed the design and fabrication processes of the experimental setup, especially a device to achieve a uniform compression force in the electrosurgical tissue welding process, as well as the procedures for sensor calibration and comparison experiments. The designed device has two parallel insulation blocks with the jaws attached to provide consistent and uniformed compression force. A setup for traditional bipolar forceps was also developed, so that the influence of force uniformity can be analyzed.

CHAPTER 4. RESULTS AND DISCUSSION

4.1 Introduction

In this chapter, data collected during the experiments are processed and analyzed. The calibrations of the force sensors are conducted and the results discussed. Force measurements show satisfactory repeatability. The fluctuation of force during the welding cycle reveals the process of tissue being heated up and loss of water content. The voltage and current data are analyzed to investigate the influences of uniform and non-uniform compression forces.

4.2 Force Sensor Calibration

The force measurements for the uniform compression case are shown in Table 4.1. The relationship between voltage reading and the applied force in Newton was found using MATLAB polyfit function as:

$$F = (677.6429 \times V + 223.09) \times 0.0098 \quad (4.1)$$

where V is the voltage reading from the force sensor and F is the corresponding force applied. The regression result is shown in Figure 4.1, with the error bars show +/- one standard deviation.

Table 4.1 Force sensor calibration for the uniform compression force device

	Voltage Reading (V)					
Applied Force (N)	**Run 1**	**Run 2**	**Run 3**	**Run 4**	**Mean**	**Standard Deviation**
6.47	0.674	0.665	0.692	0.696	0.681	0.015
9.41	0.995	1.01	1.125	1.145	1.068	0.078
15.02	1.825	1.855	1.960	1.975	1.904	0.075
22.86	3.010	3.100	3.145	3.240	3.124	0.096

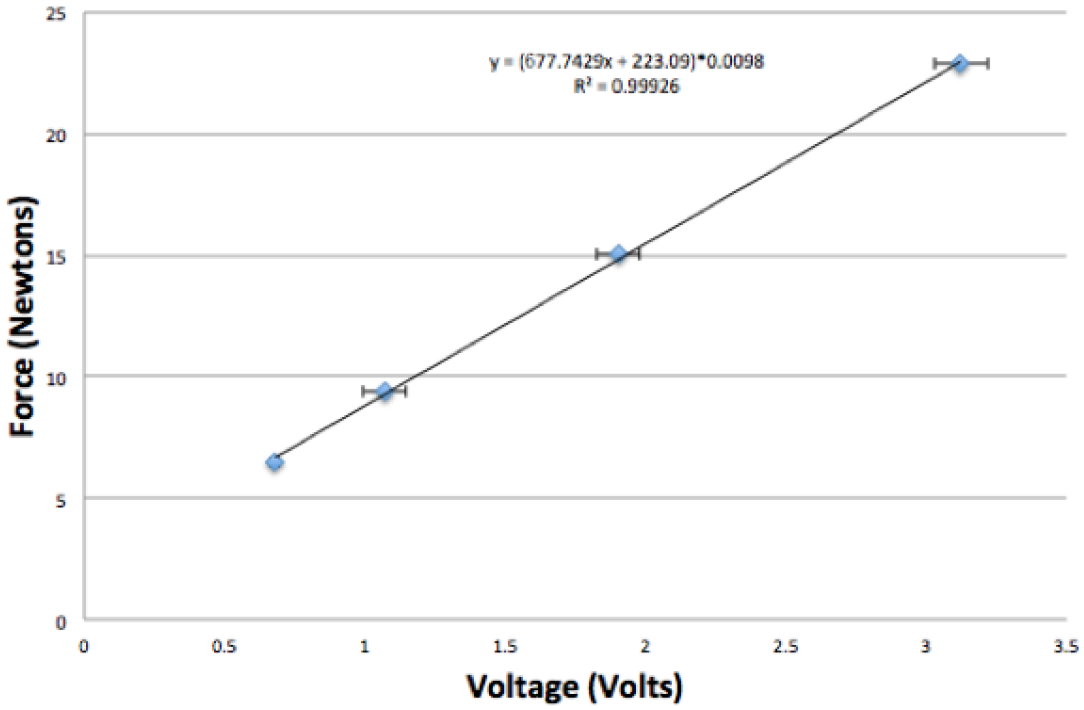

Figure 4.1 Plot of regression result for the uniform compression force case

The raw data for traditional bipolar forceps is shown in Table 4.2. Polyfit generated a function as follow:

$$F = (1672.1 \times V + 275.5) \times 0.0098 \quad (4.2)$$

The curve fits do not include zero loads and zero voltage based on the calibration processes provided by the sensor manufacturer. Figure 4.3 shows the regression plot for the data in Table 4.2, with the error bars show +/- one standard deviation.

Table 4.2 Force sensor calibration for traditional bipolar forceps

	Voltage Reading (V)							
Applied Force (N)	**Run 1**	**Run 2**	**Run 3**	**Run 4**	**Run 5**	**Run 6**	**Mean**	**Standard Deviation**
6.47	0.278	0.225	0.3325	0.263	0.338	0.275	0.285	0.043
9.41	0.387	0.319	0.467	0.422	0.518	0.392	0.417	0.069
11.37	0.464	0.397	0.616	0.512	0.625	0.481	0.516	0.089
15.02	0.6	0.574	0.852	0.77	0.778	0.635	0.701	0.113

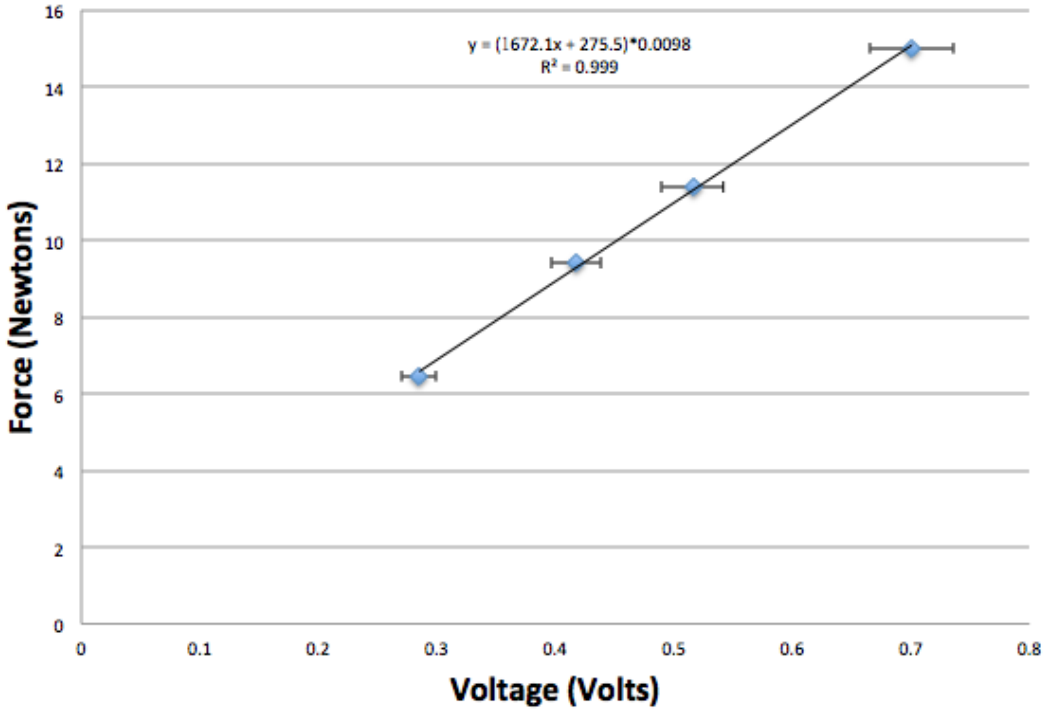

Figure 4.2 Plot of regression result for traditional bipolar forceps

The calibration of the sensor used for the non-uniform compression case was repeated six times instead of four, because the repeatability was not as good. After the calibration of the force sensor, the relationship between the force at the moving clamp and the jaws were recorded and correlated, as shown in Table 4.3. For the force sensor could not measure the force directly at the jaws during welding, the force recorded at the vise was used as the indicator for whether the target force was reached between the jaws.

Table 4.3 Correlation between the forces at the jaws and vise

Force Recorded at the Jaws (N)	Corresponding Force at the Vise (N)
5	17
8.5	64
10.5	83

These force levels at the jaws in Table 4.3 were selected based on the actual compression force achieved between the jaws in the uniform compression case. In order to achieve those force levels between the jaws, standard weights of 6.47 N, 9.41 N and 14.31 N had to be applied. The friction forces between the upper isolation block and the inner ejector pins, as well as the weight holders and the outer ejector pins, decreased the compression force at the jaws.

For traditional bipolar forceps, the compression force across the jaws is not uniform. A measurement of the force across the jaws was conducted in order to understand the force distribution. The maximum force at the tip was used as the target force level. Keeping the force reading at the moving clamp constant, the other force sensor was moved across the jaws from the tip to end manually. Forces at three points were recorded to show the non-uniformity of the force.

Figure 4.3 shows the force profile across the jaws for the 10.5 N target force, with 10 N reading at one end, the middle of the jaw recorded 8.9 N and the tip 6.5 N. For the other two force levels, the profiles measured as 8.6, 7.5, 5.3 N and 5.6, 4.8, 4.3 N, respectively. This force variation is shown in Figure 4.4. It shows that the higher the applied force, the larger the difference from the tip to the end of the jaws. Chen [21] has shown that the burst pressure of sealed vessels was different by 300 mmHg with compression forces of 10 N and 5.6 N. The force variation on the jaws found in this study shows that the uniformity of force is an important factor, which needs to be considered for the design of bipolar forceps.

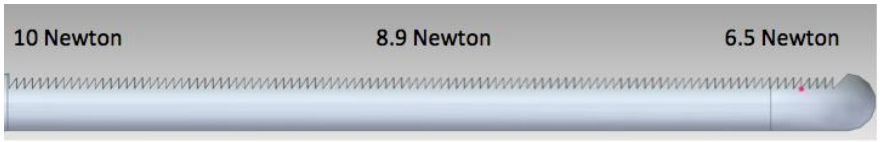

Figure 4.3 Force profile across the jaws with traditional bipolar forceps

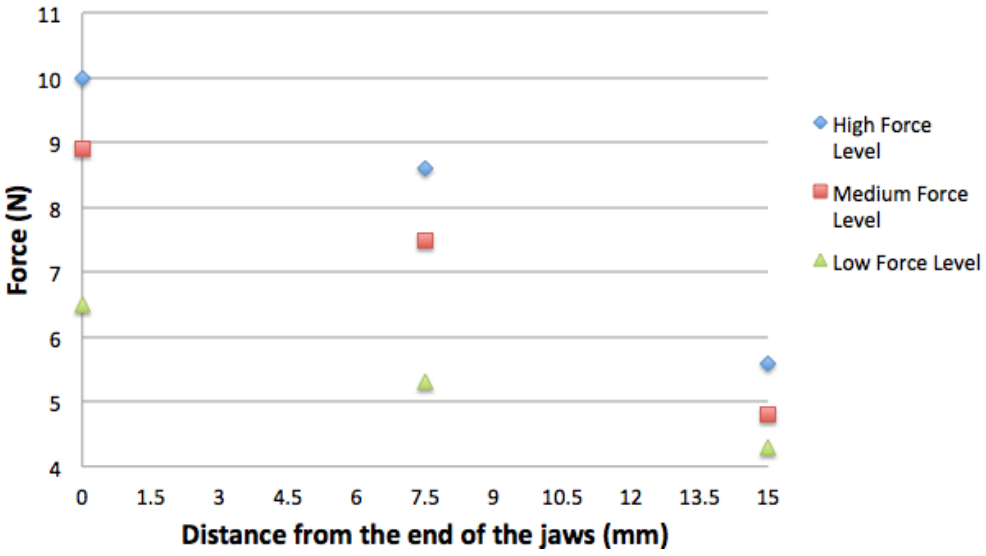

Figure 4.4 Force variation along the jaws

4.3 Forces during Welding

Real-time force measurements for the uniform compression case are presented in Figures 4.5-4.7. The two solid lines on each plot indicate the start and the end of the welding process, which are at 10 second and 25 second, respectively. At the low force level, the initial compression force for three repeated tests was about 5.7 N. After 10 seconds of recording, the welding power was turned on. The peak of the force was reached almost immediately due to the fast vaporization of water within the tissue mimic, which led to a large expansion that produced a dynamic force against the lower insulation block. Meanwhile, the upper insulation block was also raised for

a short distance. The sudden drop of the force after the peak was because that the tissue mimic became thinner after losing water, while the upper insulation block did not follow immediately due to friction. The trough of the force was the point that the upper block started to fall back to the lower block. The upper block slowly sliding back to the lower block and eventually reached the steady state where the force reading was nearly the same as the initial level.

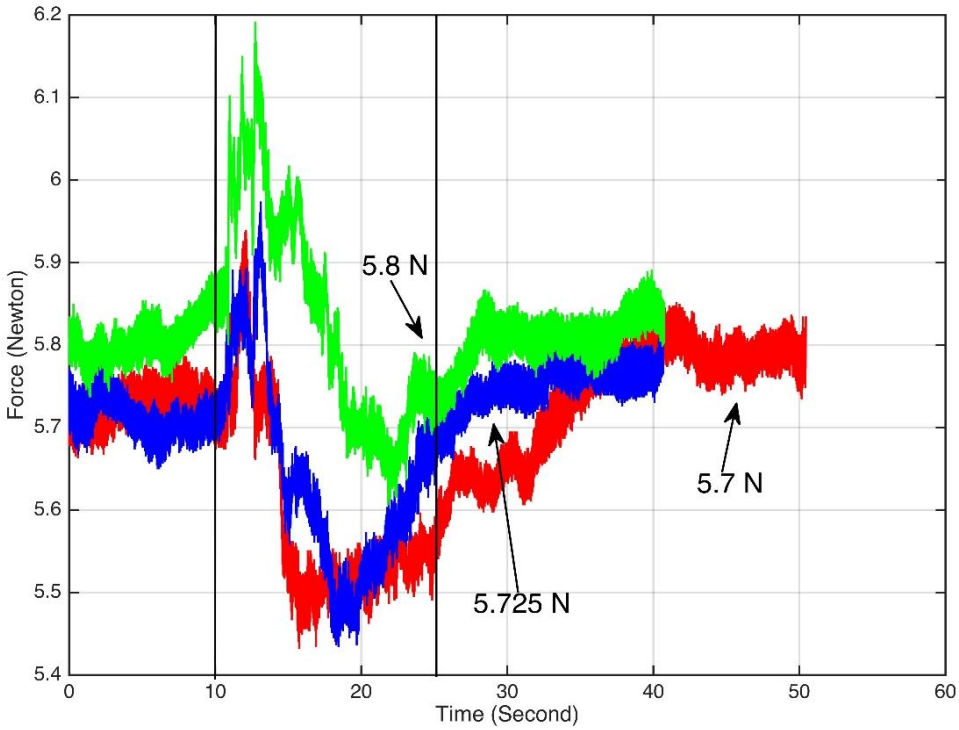

Figure 4.5 Real-time force at the low force level (6.47 N setting)

At the medium force level, the initial compression forces for the three repeated tests were 8.66, 8.85 and 9.05 N, respectively. The change of phantom material during the welding process at the medium force level was different from the low force level. The 9.05 N and 8.66 N initial force cases showed typical force fluctuation during welding. The medium level force was large enough compared to the force generated due to the vaporization of water. The force would increase due to the initial

expansion, but it was too small to lift the upper insulation block. The position of the upper block did not change, so that the peak force could be detected but there was not much force decrease after the peak. As for the case of 8.85 N, the difference could be caused by the variation of the phantom material. The material used in this test may contained a blister, which led to the first peak and quick drop of the force reading, while the larger compression force resulted in a quicker drop compared to the low level force case. The position of the upper block also changed comparing the initial and end force levels. The second peak could be caused by continuous vaporization of water content in the phantom material, for the peak was recorded at the point the footswitch was released. That means that the force stopped increasing after the power was turned off. The fact that there was a large drop in force in the 8.85 N case indicates that there could be an expulsion happened during the welding.

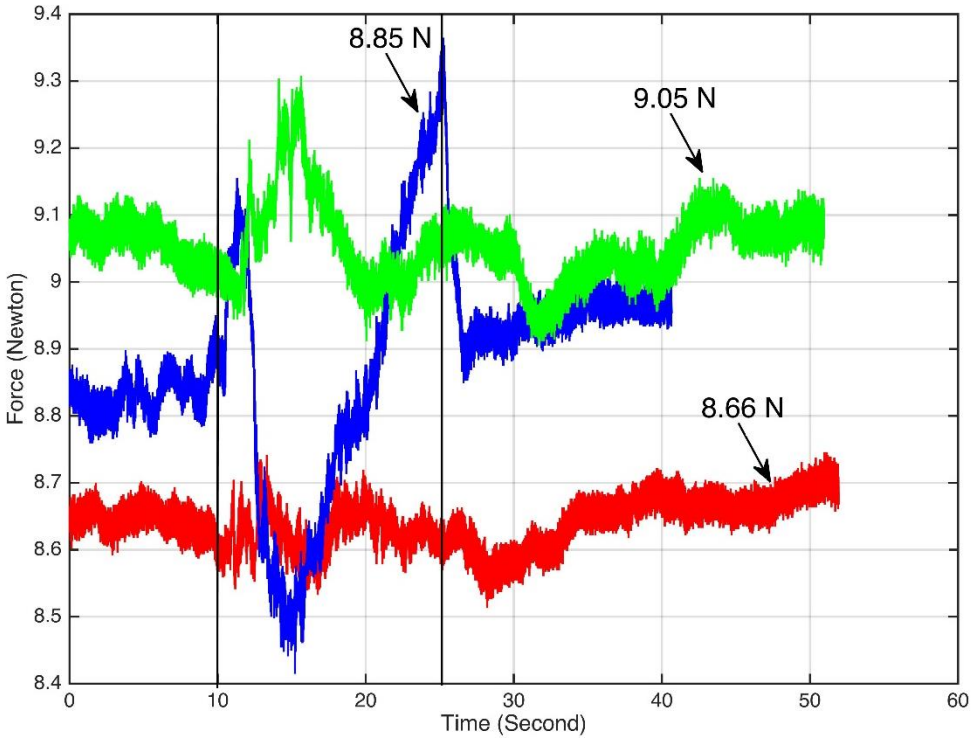

Figure 4.6 Real-time force at the medium force level (9.41 N setting)

At the high force level, the initial compression forces for the three repeated tests were 10.4, 10.6 and 10.7 N with a target force setting of 14.31 N. At the high level of force the initial force readings were not the actual steady state reading. After the force reading reached a steady state at the high force level, the jaws normally had cut through the material, which caused a short circuit and no tissue welding could be performed. All the initial readings were started just after the loading was applied. According to Figure 4.7, the post application cycle steady state readings were around 11.7 N, which shows good repeatability of the device. What happened during the application cycle was similar to the low force level case: expansion of phantom material due to the vaporization of water content, peak reached with upper block start to fall back to the lower block, and reaching steady state in the end.

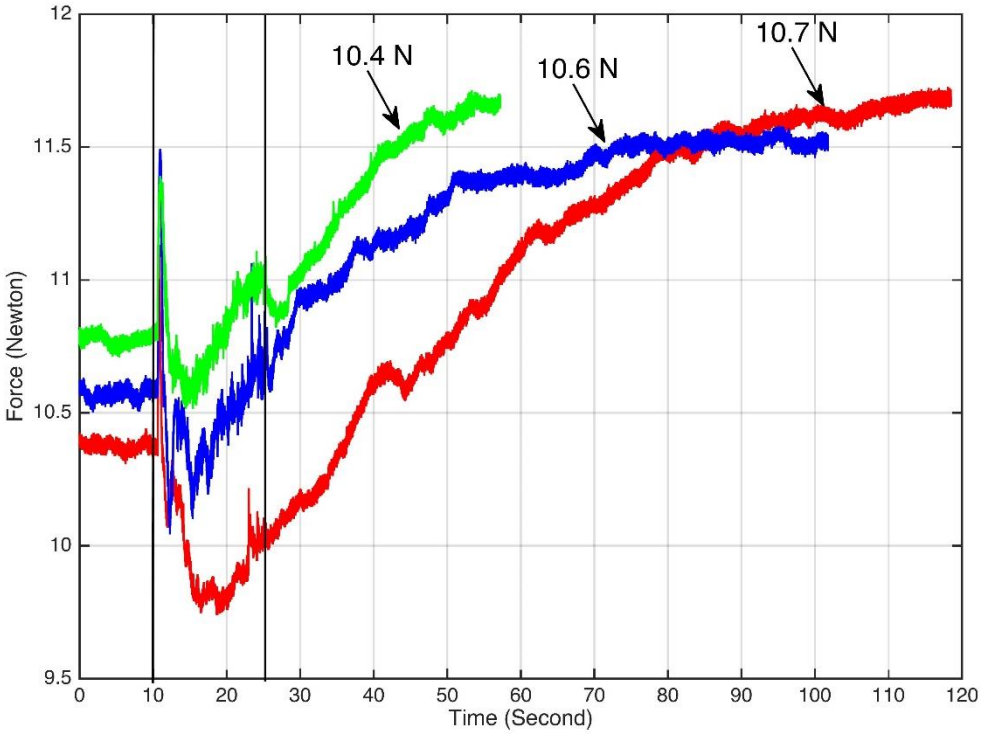

Figure 4.7 Real-time force at the high force level (14.3 N setting)

4.4 Voltage and Current Measurements during Welding

Figures 4.8-4.13 show the voltage and current comparison between designed device and traditional bipolar forceps with three different force levels. Only the peak and trough values of each sinusoid were plotted. Figures 4.8-4.10 show that at low and medium force levels, the current of the designed device is higher than the traditional bipolar forceps, while at the high force level they are similar to each other with the uniform compression case slightly less by 0.3-0.4 A. For the main function of the bipolar forceps, which is to perform tissue welding and achieve hemostasis in blood vessel, the higher current under the same power setting will lead to more heat generation within the same amount of time due to

$$\mathrm{U} = I^2 R \tag{4.3}$$

Then vessel operated with higher current would be sealed faster than lower current with the same power setting. This shows promising practical future of bipolar forceps with the uniform compression force feature. Shorter duration will also lead to lower risk of tissue charring and sticking to the jaws, which helps prevent reopening of sealed vessels. It leads to less operation time.

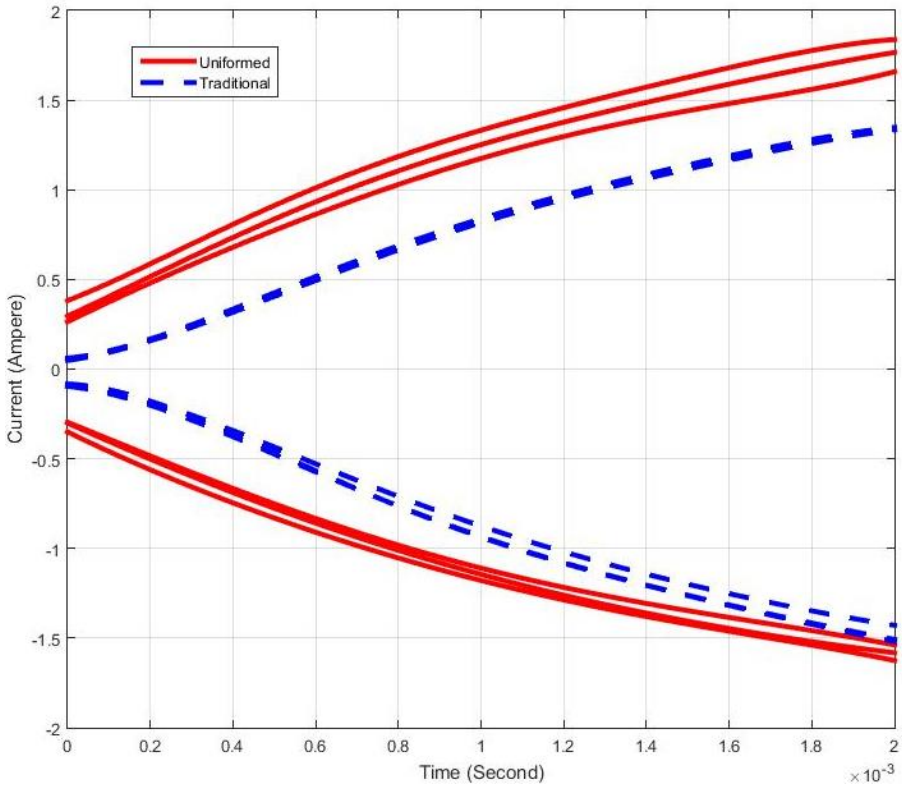

Figure 4.8 Current comparison at low force level

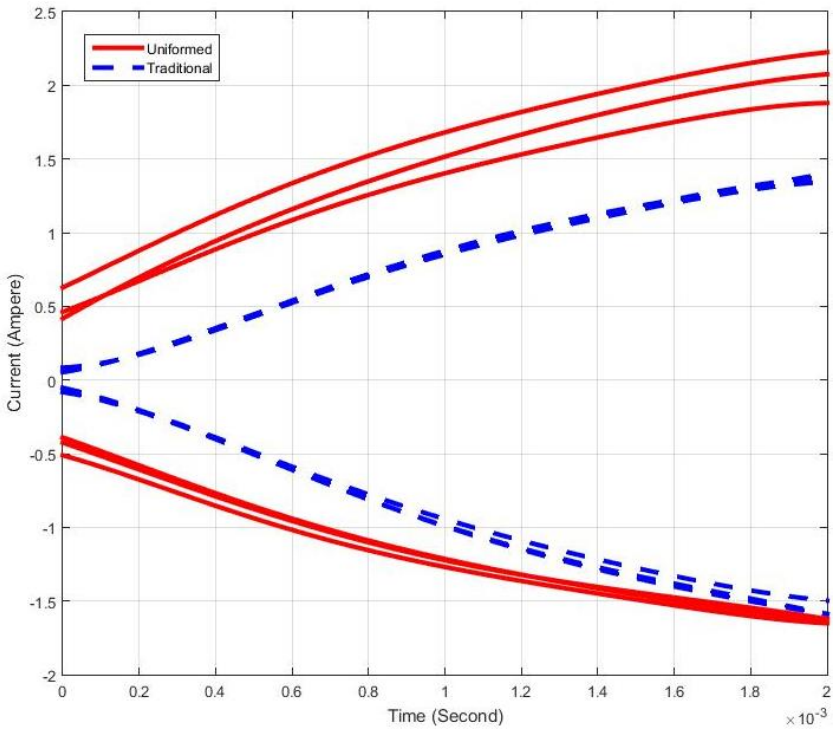

Figure 4.9 Current comparison at medium force level

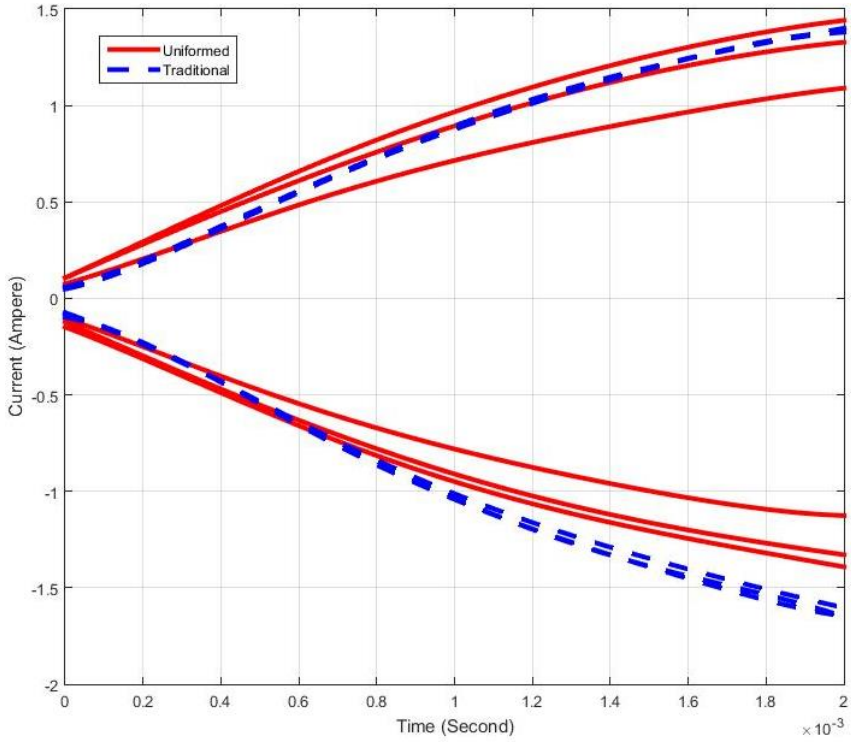

Figure 4.10 Current comparison at high force level

With the same power setting of 35W throughout the experiments, the higher current results in lower voltage at low and medium force level for the designed device. Figures 4.11-4.13 show the voltage comparison between the two devices.

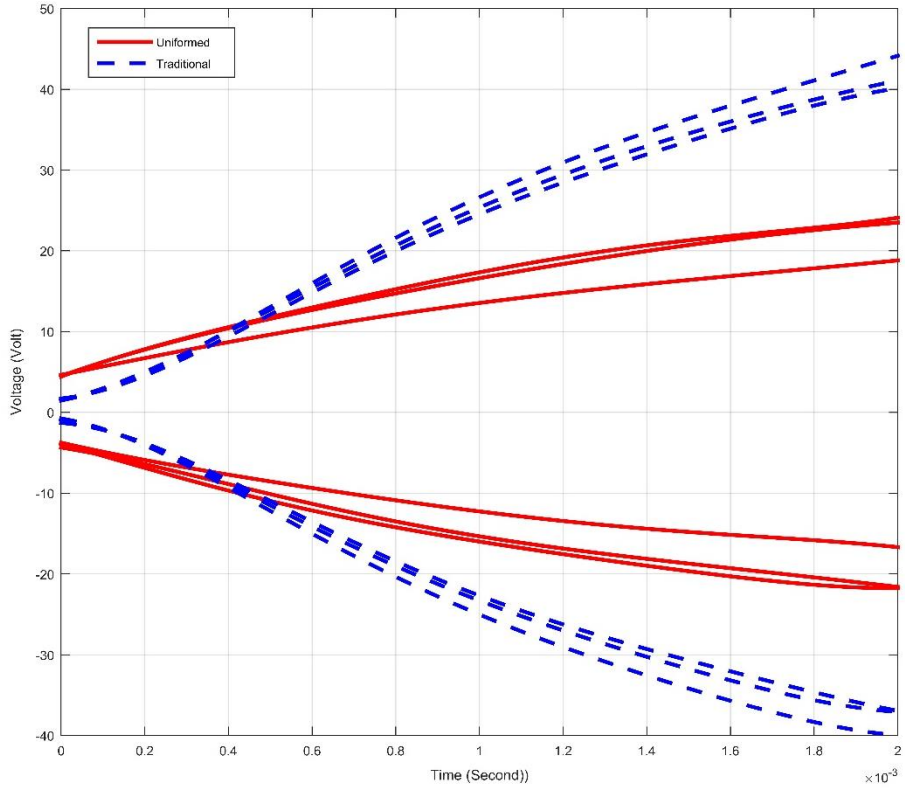

Figure 4.11 Voltage comparison at low force level

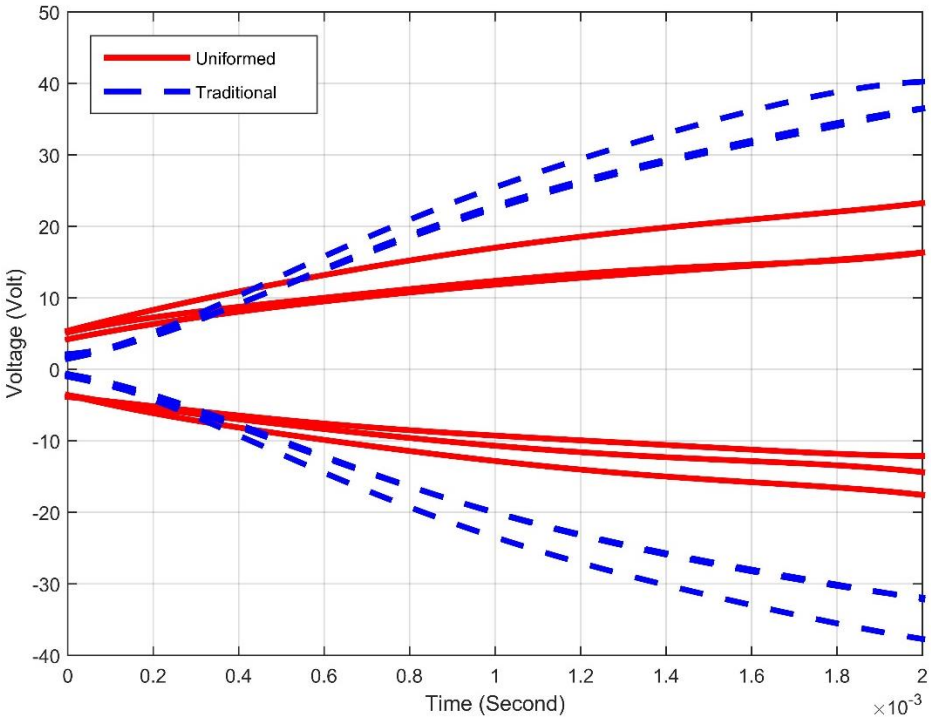

Figure 4.12 Voltage comparison at medium force level

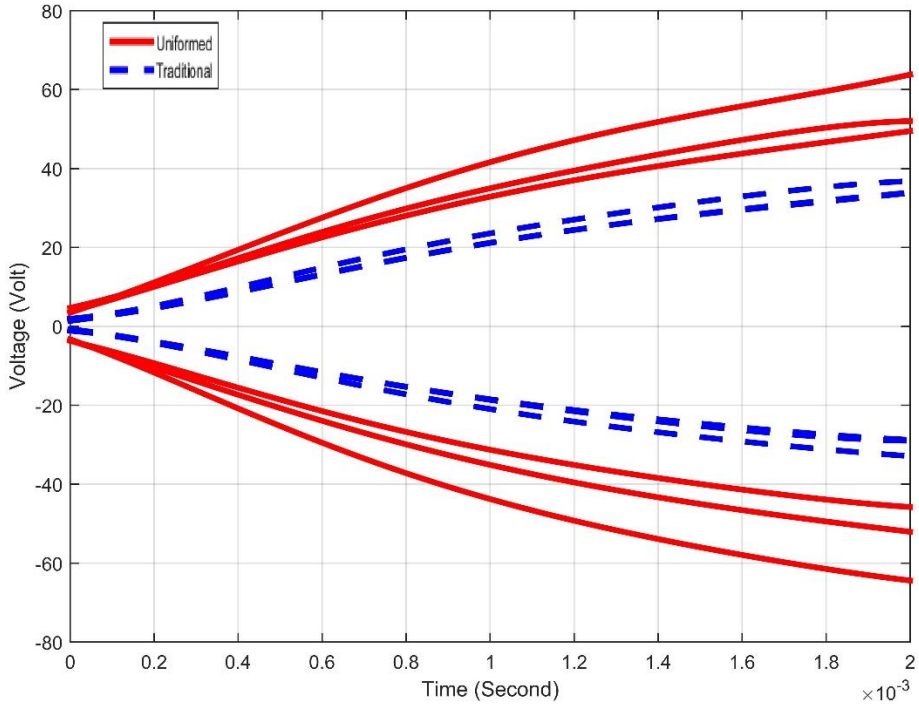

Figure 4.13 Voltage comparison at high force level

Figures 4.14 – 4.17 show how voltage and current change with different force levels in the uniform compression case and the non-uniform compression case. Figure 4.16 shows the voltages for the designed device. The medium level force generated the highest current among the three force levels. Chen also found this phenomenon [21]. Not all the vessels would have a higher burst pressure when a higher force was applied. In this case, with the same amount of welding time, the medium force level would generate the most heat compared to the other force levels, which is more likely to achieve a higher burst pressure.

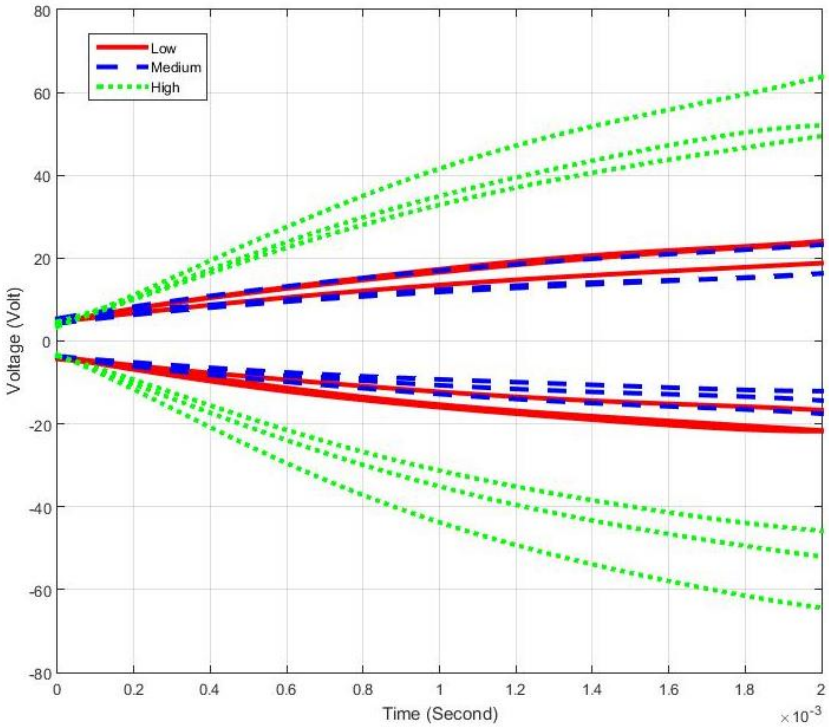

Figure 4.14 Voltage changes with different force levels for the designed device

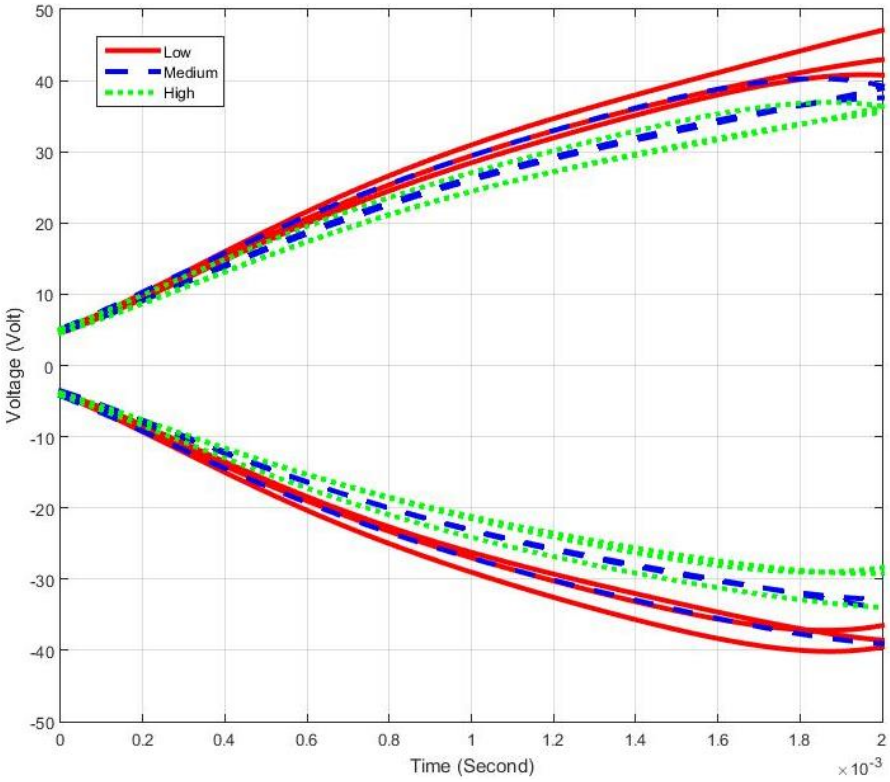

Figure 4.15 Voltage changes with different force levels for traditional bipolar forceps

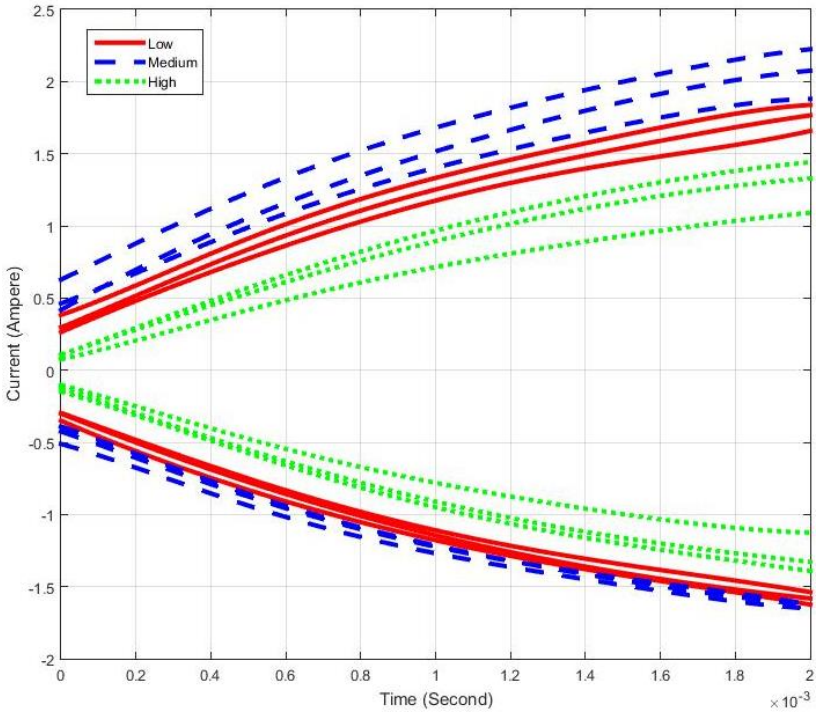

Figure 4.16 Current changes with different force levels for designed device

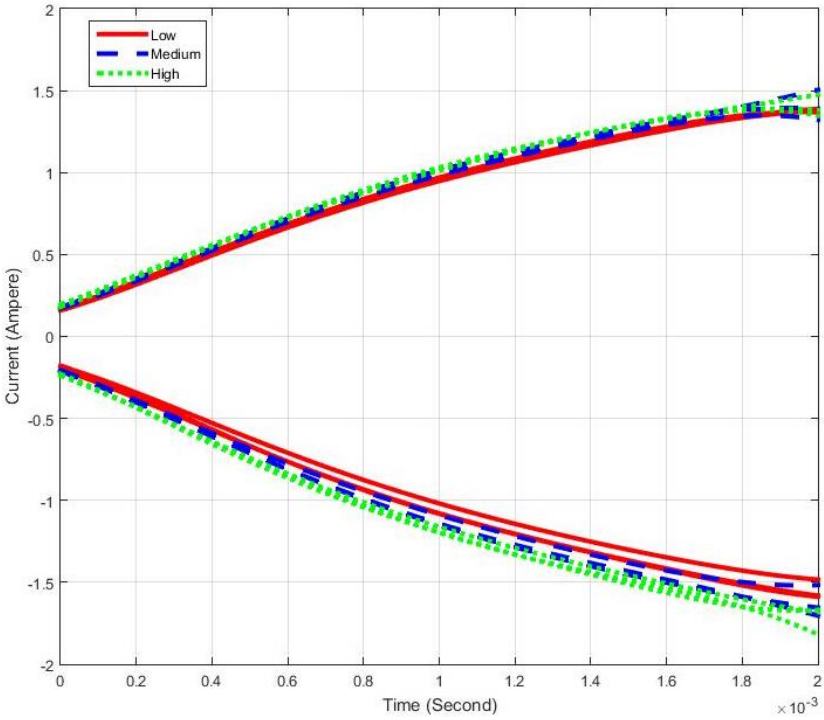

Figure 4.17 Current changes with different force levels

for the traditional bipolar forceps

4.3 Discussion

The force plots show real-time variation of compression force between the two jaws, which reveals that the changes in force during welding are significant. Based on experiments conducted, the variation of force was around 1-2 N within one welding cycle. This will lead to uncontrollable compression force during real operations. The differences may be caused by the variation of height of the upper insulation block due to the expansion and shrink of the phantom material during welding. The friction force between the insulation blocks and the ejector pins could not be eliminated completely, even after some motor lubrication oil was added during all the tests. The friction force between the lower insulation block and the ejector pins was assumed to be zero. Another uncontrollable variation was the start and end time of the welding cycle. The footswitch was manually activated and would always generate some error in starting and ending times.

The force variations within the same force level among different tests were mainly caused by the difference in the phantom material and the position of the applied weight. The blisters within the material could not be easily removed, and they may cause sudden expansion that can lead to an increase of compression force between the jaws. A better fabrication method of homogenous phantom material should be developed to reduce the measurement error. While real tissue may not contain blisters like that, a mechanism should be developed to reduced or avoid sudden increases of the compression force to reduce the risk of sticking. As for the position of applied weight, the weight holder should be improved to allow physically fixing the locations of the standard weights.

If a device with a similar mechanism as the designed device is introduced, the friction between each part should be reduced to avoid the force decreasing during the welding cycle. This would help reduce the risk of joint failure due to low burst pressure.

The insulation blocks used in the designed device could also function as a heat sink during the welding cycle since it has a higher thermal conductivity than air, such that the heat lost from the welding site is greater in the uniform compression case. Conducting a finite element (FE) simulation, such as those in COMSOL, can evaluate the influence of insulation blocks as a heat sink by using air as the surrounding material and compare the results with different insulation block materials.

During the calibration of the sensors of the non-uniform compression case, the maximum force measured across the jaws was defined as the index of the force in between. This caused errors in the comparison of the two devices. A better measurement method for the traditional bipolar forceps should be developed to reduce the effect of using the maximum force as an index.

4.4 Conclusions

With the experiment conducted in this study, it has been shown that a higher welding current can be obtained with a uniform compression force, which can lead to a shorter operation time, lower risk of tissue sticking, and less unwanted damage to surrounding tissues. The experimental setup showed good repeatability and a promising tool for further investigation on the effect of uniform and consistent compression force. The direct real-time force measurements for tissue welding

process revealed the physical process happening between the jaws during tissue welding. The understanding of current, voltage and force measurements could be the foundation of designing a compression force monitor for tissue welding quality.

CHAPTER 5. CONCLUSIONS AND FUTURE WORK

5.1 Summary and Conclusions

Electrosurgical devices are more and more widely applied in surgical procedures that are important to human health and quality of life. Ease of use, minimum side effects and better performance are just a few of the areas that the devices could be improved upon. In this research, the effect of compression force uniformity of bipolar forceps on electrosurgical tissue welding is studied. A special fixture device is designed and fabricated to achieve the parallel movement between the jaws of the bipolar forceps. Tissue welding experiments were conducted with tissue mimicking material under both uniform and non-uniform compression forces. Real-time data on force, voltage, and current were recorded with a computer-based data acquisition system and used to analyze the difference between the uniform and non-uniform compression force cases. The results indicate that the uniform compression force could potentially lead to better joint quality, reduced risk of tissue charring and sticking, and reduced operation time.

The contributions of this study can be summarized as follows:

1. Designed and fabricated a fixture device that can be used to achieve uniform and consistent compression force. This device provides an important platform for future studies in joint quality monitoring and control for bipolar electrosurgical devices.
2. Designed and conducted experiments to compare tissue welding processes under the uniform compression force case and non-uniform compression force case. This comparison has never been done before.

3. Discovered based on the experimental study conducted in this research that the uniform compression force can lead to a higher welding current, which may in turn help reduce the operation time, tissue sticking, and damage to the surrounding tissue.
4. Revealed for the first time the compression force behavior during tissue welding using bipolar electrosurgical devices.

5.2 Recommendations for Future Work

Two major side effects that need to be reduced in modern ESDs are thermal damage to adjacent tissues and tissue charring and sticking to electrodes. One potential in developing the ESD technology is to make it "smart". More real-time feedback and measurements are needed for the benefit of accurate thermal management. A smart thermal management system is needed in the future development of ESDs. The ESD should be able to generate a thermal profile throughout the operation site. At the same time, a controlled distribution of thermal energy should be achieved to avoid thermal damage to surrounding tissue.

A compression force management system can help achieve better thermal management. Influences of the compression force on thermal and electrical properties of tissue have been studied; however, the correlation between the compression force and joint quality has not been fully understood. In modern ESDs, the compression force is not measured directly or used as an input into the generator control, while it has been shown to be an important factor affecting the quality of tissue joints. A smart compression force management system could be developed to optimize the

compression force so that the force input from the operator could be reduced while achieving the optimal joint quality.

Another research need is related to tissue sticking to the electrodes. Tissue sticking is a challenging topic. Mikami attempted to quantify the sticking by measuring the time needed to clean the jaws after each operation by ultrasonic rinsing. Other methods for quantifying tissue sticking include analysis of how much protein is contained in the sticking tissue, determining the easiness to remove the sticking tissue, and even visual examination of the adhesion [7, 18, 19]. There could be signals to detect on-set sticking, including electrical, sonic, and thermal signals. The signal could then be used to prevent sticking from happening.

REFERENCES

[1] Wang, K., & Advincula, A. P. (2007). “Current thoughts” in electrosurgery. International Journal of Gynecology & Obstetrics, 97(3), 245-250.

[2] Massarweh, N. N., Cosgriff, N., & Slakey, D. P. (2006). Electrosurgery: history, principles, and current and future uses. Journal of the American College of Surgeons, 202(3), 520-530.

[3] Malis, L. I. (2006). Electrosurgery and bipolar technology. Neurosurgery, 58(1), ONS-1.

[4] Untitled photograph of bipolar forceps, retrieved on Nov 17th, 2014 from: http://img.medicalexpo.com/images_me/photo-g/bipolar-forceps-electrosurgial-unit-bayonet-titanium-68645-107357.jpg
and http://www.gentek.com.tr/storage/images/bulent/bipolar_kafa.jpg

[5] Vilos, G. A., & Rajakumar, C. (2013). Electrosurgical generators and monopolar and bipolar electrosurgery. Journal of minimally invasive gynecology, 20(3), 279-287.

[6] Hendrickson D. Minimally invasive surgery: evidence based ligation and hemostatic techniques. Proceedings of the American College of Veterinary Surgeons Symposium. Washington, 2012.

[7] Mikami, T., Takahashi, A., Hashi, K., Gasa, S., & Houkin, K. (2004). Performance of bipolar forceps during coagulation and its dependence on the tip material: a quantitative experimental assay: Technical note. Journal of neurosurgery, 100(1), 133-138.

[8] Konesky, G. (1998), Porosity Evolution in Electrosurgical Blade Coatings. MRS Proceedings, Cambridge Univ Press.

[9] Ou, K.-L., et al. (2014). "Biomedical nanostructured coating for minimally invasive surgery devices applications: characterization, cell cytotoxicity evaluation and an animal study in rat." Surgical endoscopy: 1-15.

[10] Ceviker, N., et al. (1998). "A new coated bipolar coagulator: technical note." Actaneurochirurgica**140**(6): 619-620.

[11] Oberdorster G, Gelein RM, Ferin J, Weiss B (1995) Association of particulateair pollution and acute mortality: involvement of ultrafine particles? InhalToxicol 7:111–124

[12] Vellimana, A. K., et al. (2009). "Current technological advances of bipolar coagulation." Neurosurgery**64**(3): ons11-ons19.

[13] Rioux, J.-É. (2007). "Bipolar electrosurgery: a short history." Journal of minimally invasive gynecology**14**(5): 538-541.

[14] Bulsara, K. R., et al. (2006). "History of bipolar coagulation." Neurosurgical review**29**(2): 93-96.

[15] Munro, M. G. (2012). Fundamentals of electrosurgery Part I: Principles of radiofrequency energy for surgery. In *The SAGES Manual on the Fundamental Use of Surgical Energy (FUSE)* (pp. 15-59). Springer New York.

[16] Kennedy, J. S., Stranahan, P. L., Taylor, K. D., & Chandler, J. G. (1998). High-burst-strength, feedback-controlled bipolar vessel sealing. *Surgical endoscopy*, *12*(6), 876-878.

[17] Dodde, R. E. (2011). *Bioimpedance of soft tissue under compression and applications to electrosurgery* (Doctoral dissertation, The University of Michigan).

[18] Richter, S., Kollmar, O., Schilling, M. K., Pistorius, G. A., & Menger, M. D. (2006). Efficacy and quality of vessel sealing. *Surgical Endoscopy And Other Interventional Techniques*, *20*(6), 890-894.

[19] Broughton, D., Welling, A. L., Monroe, E. H., Pirozzi, K., Schulte, J. B., & Clymer, J. W. (2013). Tissue effects in vessel sealing and transection from an ultrasonic device with more intelligent control of energy delivery. *Medical devices (Auckland, NZ)*, *6*, 151.

[20] Chastagner, M. W. (2010). *Investigation of electrosurgical tissue joining*(Doctoral dissertation, The University of Michigan).

[21] Chen, R. K., Chastagner, M. W., Geiger, J. D., & Shih, A. J. (2014). Bipolar Electrosurgical Vessel-Sealing Device With Compressive Force Monitoring.*Journal of biomechanical engineering*, *136*(6), 061001.

[22] [Untitled photograph of bipolar forceps]. Retrieved Apr. 15th, 2015, from: http://vet.uga.edu/mis/equipment/energy.php and http://www.dalcross.com.au/media/pics/site/imagecache/0/4/04ECF9C83065984EC71A70EC983DE0C6.jpg

[23] Prospector, Typical Properties Generic PEI. http://plastics.ulprospector.com/generics/28/c/t/polyether-imide-pei-properties-processing

[24] Tekscan, Can I trim flexiforce sensor? https://www.tekscan.com/support/faqs/can-i-trim-flexiforce-sensor

[25] Chen, R. K., & Shih, A. J. (2013). Multi-modality gellan gum-based tissue-mimicking phantom with targeted mechanical, electrical, and thermal properties. *Physics in medicine and biology*, *58*(16), 5511.